

Network Bypasses Sustain Complexity

Ernesto Estrada^{1*}, Jesús Gómez-Gardeñes^{2,3†}, Lucas Lacasa^{1‡}

¹Institute for Cross-Disciplinary Physics and Complex Systems (IFISC)
CSIC-UIB, Palma de Mallorca, Spain

²Department of Condensed Matter Physics, University of Zaragoza, E-50009 Zaragoza, Spain

³GOTHAM Lab – Institute for Biocomputation and Physics of Complex Systems (BIFI)
University of Zaragoza, E-50018 Zaragoza, Spain

July 3, 2023

Abstract

Real-world networks are neither regular nor random, a fact elegantly explained by mechanisms such as the Watts-Strogatz or the Barabási-Albert models, among others. Both mechanisms naturally create shortcuts and hubs, which while enhancing network's connectivity, also might yield several undesired navigational effects: they tend to be overused during geodesic navigational processes –making the networks fragile– and provide suboptimal routes for diffusive-like navigation. Why, then, networks with complex topologies are ubiquitous? Here we unveil that these models also entropically generate network bypasses: alternative routes to shortest paths which are topologically longer but easier to navigate. We develop a mathematical theory that elucidates the emergence and consolidation of network bypasses and measure their navigability gain. We apply our theory to a wide range of real-world networks and find that they sustain complexity by different amounts of network bypasses. At the top of this complexity ranking we found the human brain, which points out the importance of these results to understand the plasticity of complex systems.

*estrada@ifisc.uib-csic.es

†gardenes@gmail.com

‡lucas@ifisc.uib-csic.es

1 Introduction

The advent of Network Science [1, 2] was marked by the urgent need to decipher simple and local mechanistic models underlying the self-organized formation and growth of natural and artificial real-world networks, models able to parsimoniously account for large-scale structural patterns systematically deviating from stylized ones such as purely ordered lattices or purely random graphs. Two such celebrated models, aiming to explain the ubiquitous real-world patterns of “small-worldness” (SW) and “scale-freeness” were proposed in seminal contributions by Watts and Strogatz [3] and Barabási and Albert (BA) [4], respectively. The resulting network topologies of SW and BA networks –poised between order and disorder at the statistical level– were coined as ‘complex’. Here we give a special attention to these as they are paradigmatic mechanisms that create complexity through heterogeneization, although we acknowledge that other patterns [2] –e.g. communities, assortative and disassortative mixing, triadic closure, etc– are also relevant in this context.

Indeed, what is complex in a complex network? Conceptually, system complexification [5] may occur via different types of mechanisms including symbiosis, exaptation or structural deepening to cite some. The latter concept of structural deepening [6], which we adopt here, focuses on the situation where the efficiency of an existing function in the system is increased as the system complexifies, where a higher efficiency is usually interpreted in terms of performing the same function using less available energy. Accordingly, a network with a structure poised between total order (lattice) and pure disorder (random graph), such as SW and BA networks as well as many networks in the real-world, is compatible with the existence of a structural deepening mechanism which improves the communication efficiency between the nodes in the networks. Identifying a quantitative proxy that characterizes such structural deepening mechanism in net-

works remains, however, an open problem, and constitutes the first motivation of this work. As a matter of fact, the Watts-Strogatz mechanism does not provide a clear-cut definition of what a SW network is –only a certain range of network’s mean path length and clustering coefficient–, indicating that neither of these two network properties are quantitative proxies of a potential structural deepening mechanism. Similarly, the extensive zoology of degree distributions existing in empirical networks [7, 8] points to the fact that observing scale-freeness is not in itself enough to indicate the existence or not of a structural deepening mechanism. Other network properties, such as the node-based fractal dimension (NFD), the node-based multifractal analysis (NMFA), the structural distance, or the degree of complexity [9, 11] suffer from similar problems, and e.g. fail to identify a specific point within the SW region where structural deepening is maximized.

And yet, networks serve the purpose of facilitating the communication between otherwise isolated entities of a complex system. Therefore, if a structural deepening mechanism exists in the evolution of a network it is likely that it involves an improvement of some communication efficiency. SW and BA-type mechanisms indeed tend to generate networks with enhanced connectivity [9] (a form of structural deepening) which are robust against random failures [10, 11], what in principle could explain the ubiquity of these mechanisms and the resulting macroscopic patterns, even if quantifying such complexity has proven elusive.

However, observe that the SW mechanism reduces mean path length simply by creating path shortcuts, making enhanced connectivity overly dependent –and thus, fragile– on them. Likewise, in BA-like networks, shortest paths often involve hubs, and these networks are known to be extremely fragile against failure of hubs [19] or jamming [20, 21, 22, 23], potentially inducing a failure cascade which can severely harm the macroscopic network’s function.

Why, then, complex networks are ubiquitously observed? First, note that walkers navigating a network do not necessarily have full information of the network structure, and geodesic navigation is indeed a global optimization problem [68] that, accordingly, “blind” walkers cannot perform. Second, such blind walkers typically undergo diffusion-like navigation and such parsimonious navigation strategy can lead walkers to ‘diffuse out’ and get lost easily if attempting to follow shortest paths, as these tend to have higher degree nodes¹. Accordingly non-geodesic navigational strategies have been proposed [12, 13, 14, 15, 16, 17, 18], usually providing heuristic recipes based on local network information available (such as the degree [12, 13, 14] or the matching index [15]). Solving the apparent dilemma between the prevalence of complex network architectures –underpinned by WS and BA mechanisms among others– with structural deepening related to enhanced communication capacity requires to find parsimonious mechanisms which can mitigate the undesired effects of geodesic navigability, and this is the second motivation of our work.

Our contention in this work is that as a network complexifies, it is capable to mitigate the impact of the undesired geodesic navigability issues by structural deepening mechanisms which favor the consolidation of network bypasses: alternative routes to mere geodesic navigation that (i) decrease the tendency of ‘getting lost’ by blind walkers, and (ii) if needed, can also be used by non-blind walkers to avoid problematic links and nodes, therefore allowing the overall connectivity to be maintained and the network to be robust against failure of shortcuts and hubs.

¹A node of degree k potentially connects $k(k - 1)/2$ pairs of nodes by shortest paths of length two. Longer SP also use them to connect other pairs of nodes. Thus, the higher the degree of a node the higher the number of SP crossing that node.

In what follows we start from first principles and develop a theory to define and detect the emergence of network bypasses in both synthetic and real-world networks, and quantify their associated gain and impact in terms of network navigability. Our theory is based on a network geometrization by which initially unweighted edges and paths acquire an effective weight –an effective length, or cost– induced solely by the topology of the surrounding network’s structure. Network bypasses then emerge as geodesic paths in the geometrized network (i.e. they are the solutions of a new type of topology-induced minimum-cost path optimization problem [36]), and in many cases we show they don’t coincide with the shortest paths of the original network. We also show that (i) the emergence of these network bypasses is an unavoidable (entropic) byproduct of the WS and BA mechanisms themselves, and that (ii) the effect of these bypasses is optimally emphasized when networks fall in a specific point of SW regime and an intermediate edge density in the sparse regime for BA-like networks, thus finding a quantitative proxy for structural deepening. We also certify that (iii) network bypasses indeed provide source-destination routes with better navigation properties for diffusive-like blind walkers than geodesic routes, and finally rank and discuss the emergence of network bypasses and their associated navigability gain in a range of real-world networks.

2 Results

To fix the intuition, let us begin by illustrating two situations in simple graphs that highlight the importance of bypasses in the operation of a network that harbors transportation and propagation of signals and information. To this aim, we initially consider a particle hopping between the nodes of a network created via the WS model [3], and we focus on the propagation of the particle between nodes i and j (see Panel (a) in Fig. 1). Starting with rewiring probability $p = 0$ we have a circulant graph \mathcal{G} , and the path $P_1 = \{i, j - 1, j\}$ of length 2 (highlighted in blue) is

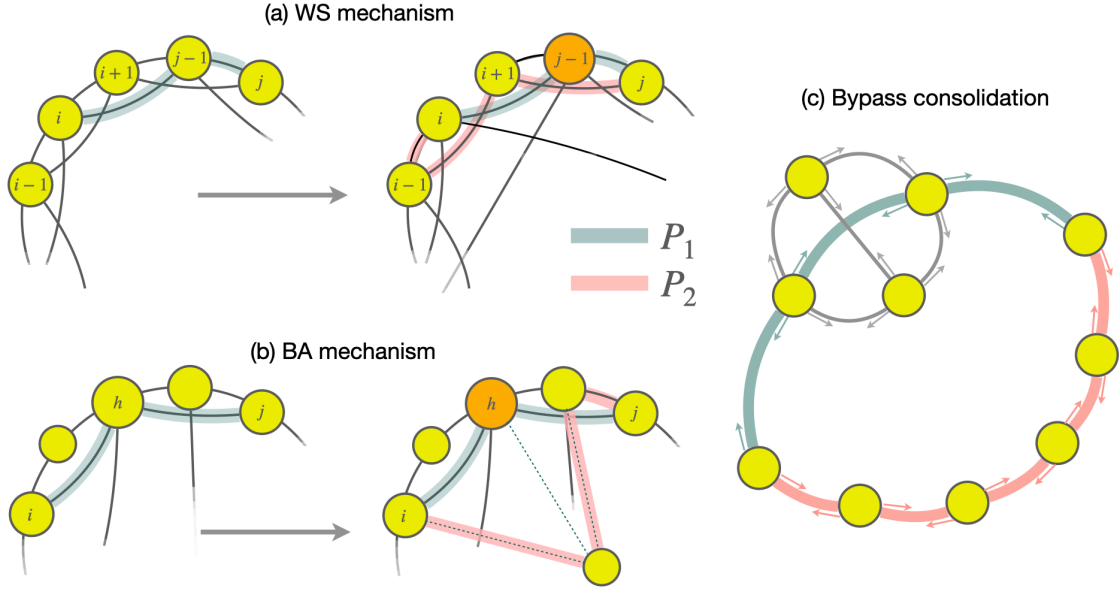


Figure 1: (Panel a) Illustration of the effects of the edge rewiring process in the Watts-Strogatz model on the paths connecting two arbitrary vertices of the resulting graph: the shortest path P_1 (blue) can be bypassed by the path P_2 (pink), topologically longer but with a lower energetic cost. (Panel b) Similar phenomenon happens when the node h becomes a hub after a rich-get-richer mechanism. Shortest path P_1 (blue) typically cross the hub but, with a sufficiently large mean degree, other paths such as P_2 (pink) can bypass the shortest path P_1 , allowing alternative routes when hubs reach capacity and become saturated or damaged. (Panel c) Navigational dilemma embedded in a network: the blue path P_1 is the shortest path, but it turns out that the pink ‘braquistochronic’ path P_2 is more advantageous as it avoids congestion and is less resistive (see SI section S5 for an explicit calculation).

a shortest path connecting i and j . Mimicking the action of WS-like mechanism kicking in, the edge $e = (i, i + 1)$ of \mathcal{G} is randomly rewired, and subsequently another edge is also randomly rewired, so that node $j - 1$ now receives an edge from a ‘distant’ node. In the resulting graph \mathcal{G}' , vertex $i + 1$ drops its degree by one, whereas vertex $j - 1$ increases its degree. This situation creates a small degree heterogeneity in the graph \mathcal{G}' which did not exist in the circulant graph \mathcal{G} : node $j - 1$ now participates in many more shortest paths starting elsewhere and ending at vertex $j - 1$. Accordingly, the length-2 path P_1 , in practice, might not be the “best” route to connect i and j , even if it is still the shortest path, topologically speaking. For instance, a random walker

choosing P_1 has a higher likelihood of “diffusing out” through $j - 1$, thus hardly reaching the destination. Likewise, geodesic navigation will make $j - 1$ systematically overused, leading to a higher chance of damage or jamming. In turn, the length-3 path $P_2 = \{i, i - 1, i + 1, j\}$ (highlighted in pink), while being topologically longer than P_1 , contains node $i + 1$ whose degree is at the same time lower than the average and also avoids $j - 1$, hence can be seen as a potentially more ballistic route that avoids a potentially problematic $j - 1$ and still connects i and j .

A similar situation is depicted in Panel (b) of Fig.1 where node h becomes a hub via a rich-get-richer (i.e. BA-like) mechanism. The shortest path between i and j (highlighted in blue) will again be more prone for the walker to get lost due to the presence of a high-degree node, once the BA mechanism enhances such heterogeneity. Now, if the network supports a sufficiently large² mean degree –i.e. if the network allows more edges to be formed than a spanning tree–, then other routes can emerge, bypassing the hub (pink path).

The two examples illustrated in Panels (a) and (b) Fig. 1 raise the question of whether a particle would “prefer” to travel from i to j via the shortest –albeit with higher uncertainty to reach the destination– path P_1 or along the slightly longer but more ballistic –smaller uncertainty– alternative path P_2 . In Panel (c) of the same figure we illustrate such conundrum, where two alternative routes (a shortest path P_1 , in blue, and a topologically longer one P_2 , in pink) are highlighted. Intuition tell us that there should be a trade-off: sometimes P_1 is to be preferred, sometimes P_2 is a contingently better option. Extending this situation to a network-growth mechanism, this suggests that the creation of shortcuts (SW) and hubs (BA) should be sustained by the emergence of some alternative paths bypassing these, with structural deepening effects that would reach a maximum impact for a specific rewiring probability p (SW) as well as spe-

²yet sufficiently small so that the network is in the sparse regime

cific hub abundance (BA). In what follows we introduce a formalism that puts these questions and their general solution in a solid grounding.

The concept of *Resistive Paths*

Starting from first principles, the possible trajectories that a hopping particle can perform over a network $\mathcal{G} = (V, E)$ of $|V| = n$ nodes with binary adjacency matrix $\mathbf{A} = \{A_{ij}\}_{i,j=1}^n$ can be enumerated by computing the powers of \mathbf{A} . A natural way to penalize longer trajectories connecting the same initial and end nodes is to properly weight them

$$\mathbf{G}(\beta) = e^{\beta\mathbf{A}}; G_{ij}(\beta) = \sum_{l=0}^{\infty} \frac{\beta^l (\mathbf{A}^l)_{ij}}{l!} = (e^{\beta\mathbf{A}})_{ij}, \quad (1)$$

where β is an empirical parameter. This expression is known as the communicability function of a graph [37, 38]. While originally being a purely combinatorial expression that encapsulates the contributions of different walks in a graph, $\mathbf{G}(\beta)$ indeed emerges as a central matrix when analysing a wide variety of dynamics on graphs [38, 39, 40, 41, 42] (see SI S1.1 for details and S1.2 for a derivation of $\mathbf{G}(\beta)$ as the actual propagator in a specific case with Hamiltonian dynamics). Nowadays communicability is applied across a range of disciplines, from neuroscience [43, 44, 45, 46, 47, 48, 49, 50] or cancer research [51] to ecology [52] or economics [53], to cite a few.

While this operator naturally emerges on relation to different types of dynamics on networks, in this work we shall highlight that it is fundamentally a combinatorial one, and is not a priori derived from any concrete dynamics running on the network. In other words, while we will consider that there is some kind of generic propagation –let it be information, electrons, or other types of particles hopping through the network–, the theory presented hereafter does not require to specify which dynamical equations rule such propagation, as we focus on the structural (topological) constraints which generally affect such propagation. By analogy to the cases

discussed in SI S1.1, S1.2 and [38], we call G_{ij} the structural propagator, which parsimoniously captures the role that the network's architecture plays in j receiving particles sent from i . Similarly, G_{ii} accounts for how much a node i structurally retains an item at it, as the item returns to i infinitely often. For a particle initially located at the node i the difference:

$$R_{i \rightarrow j}(\beta) = G_{ii}(\beta) - G_{ij}(\beta) \quad (2)$$

accounts for the opposition offered by the network structure to the directional displacement of a particle sent by node i to the node j , where the smaller the value of $R_{i \rightarrow j}$, the higher the probability that the particle does not get trapped at the origin i and can propagate to node j , *i.e.*, there are more conductive walks between i and j than those returning back to the origin. In order to account for the resistance of the displacements between any pair of nodes we should take into account the two possible directions of their mutual communication ($i \rightarrow j$ and $j \rightarrow i$). To this aim, one can symmetrize (2) to define the *communication resistance* between nodes i and j as: $\xi_{ij}(\beta) := (R_{ij}(\beta) + R_{ji}(\beta))^{1/2}$. From the definition of the communicability function, and setting $\beta = 1$ without loss of generality, we obtain that the *communication resistance* reads:

$$\xi_{ij}^2 = \sum_{m=1}^n e^{\lambda_m} \left((\psi_m)_i - (\psi_m)_j \right)^2. \quad (3)$$

where $(\psi_m)_i$ is the i -th entry of the eigenvector associated to the m -th eigenvalue (λ_m) of \mathbf{A} . We rigorously proved that ξ_{ij} is an Euclidean distance (see SI section S2 for a proof). Conceptually, ξ_{ij} is a measure of the network resistance to a flow between i and j . Recently [54], it was proven that this communicability distance –and every spherical euclidean distance– is the effective resistance between nodes in a network with given edge weights.

Network Geometrization and *Resistive Shortest Paths*

Since ξ_{ij} is an Euclidean distance and particles motion is confined to the network edges, we can proceed to the geometrization of the network [55, 56]. To this aim we first transform every

edge of the graph into a compact 1-dimensional manifold. That is, for an edge $e = \{i, j\}$ we consider the boundary of the manifold to be $\partial e = i \cup j$. Then, each edge e inherits a metric g_e such that (e, g_e) is isometric to a finite interval $[0, L(e)]$ of the real line with the standard metric, where the length $L(e)$ is given by the communicability distance of the corresponding edge, i.e. $L(e) \equiv \xi_e = \xi_{ij}$. Finally, the distance metric on the edges is extended to the full graph via infima of lengths of curves in the geometrization of \mathcal{G} , such that the graph becomes a metrically complete length space [56].

Equipped with this geometrization, we can now define two different types of lengths for any given path $\mathbf{p}(s \rightarrow t) = (s, \dots, t)$ connecting nodes s and t in the network. First, the *topological length* $\ell_{\mathbf{p}(s \rightarrow t)}$ of this path is just the number of edges in it. Among all paths $\{\mathbf{p}(s \rightarrow t)\}$ connecting s and t , the one with the minimum length is denoted the shortest path $\text{SP}(s, t)$ as

$$\text{SP}(s, t) = \operatorname{argmin}_{\mathbf{p}(s \rightarrow t)} [\ell_{\mathbf{p}(s \rightarrow t)}] \quad (4)$$

Observe that Eq.4 can have more than one solution, specially for large networks (see SI S4).

Second, and based on the geometrization induced by the communicability resistance above, we also define an *effective length* $\mathbb{L}_{\mathbf{p}(s \rightarrow t)}$ by summing the induced length of each of the links involved in $\mathbf{p}(s \rightarrow t)$:

$$\mathbb{L}_{\mathbf{p}(s \rightarrow t)} = \sum_{(i,j) \in E \in \mathbf{p}(s \rightarrow t)} \xi_{ij} . \quad (5)$$

At odds with $\ell_{\mathbf{p}(s \rightarrow t)}$, which blindly assigns the same length (unity) to every edge of the network, $\mathbb{L}_{\mathbf{p}(s \rightarrow t)}$ takes into account the topological neighborhoods of each of the nodes in the path and the associated likelihood that the particle might diffuse out of the path, accordingly. Likewise, it penalises paths for which particles take naturally more time to travel due to the structure of the network in which the path is embedded in. The specific path connecting s and t that minimizes

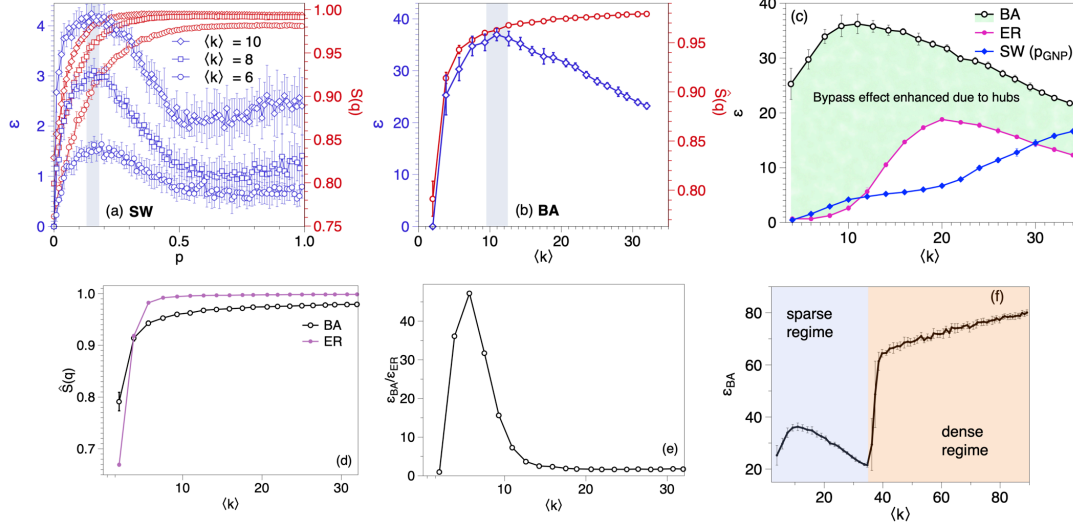


Figure 2: Plot of the normalized communicability entropy $\hat{S}(\mathbf{q})$ (red) and of the net gain factor ϵ (blue) vs. : (a) the rewiring probability p for WS networks (numerical step of $\delta p = 0.01$) with $n = 250$ nodes and different average degree $\langle k \rangle$, or (b) the mean degree $\langle k \rangle$ of a BA model with $n = 250$ nodes. Each dot is the average of 100 realizations, and standard deviations over the ensemble of realizations are also depicted. In both panels, the shaded blue area highlights the maximum of ϵ and marks the network’s Good Navigational Point ($p_{\text{GNP}} \approx 0.15$ for WS model, $\langle k \rangle_{\text{GNP}} \approx 11$ for BA model). (c) ϵ vs $\langle k \rangle$ for networks of $n = 250$ nodes generated via the BA model, the WS model (poised at the Good Navigational Point) and an Erdos-Renyi (ER) model for comparison. The bypass-induced navigability gain is substantially larger in heterogeneous (BA) networks than in more homogeneous ones (the ratio $\epsilon_{BA}/\epsilon_{ER}$ is plotted in (e) to highlight such difference). The comparison between ER and SW networks is nontrivial and can be explained in terms of the shapes of the respective degree distributions as $\langle k \rangle$ increases (see the text and SI). (d) Normalized communicability entropy of both BA and ER networks with the same number of nodes, as a function of the mean degree. (f) ϵ_{BA} vs $\langle k \rangle$ in the extended region of high density, where preferential attachment is not properly working anymore (see SI S9), leading to an explosion of the navigability gain due to the transition to ultra-short graphs.

this effective length is denoted the *Shortest Resistive Path* $\text{SRP}(s, t)$, defined as:

$$\text{SRP}(s, t) = \operatorname{argmin}_{p(s \rightarrow t)} [\mathbb{L}_p(s \rightarrow t)]. \quad (6)$$

We are now ready to quantify (i) the emergence of potential bypasses –i.e. the proliferation of non-SP between any two nodes– and (ii) decide in a principled way when this path redundancy become relevant to the network function –something that, we advance, will happen when SRPs start to differ from SPs–.

Communicability Entropy

To address the first question above we now quantify, both microscopically and then at the network level, the degree by which, as disorder increases, new routes between edges become available. To this aim, let us return to the WS and BA models that we have considered before. As we have discussed, both the rewiring process and the BA mechanism create degree heterogeneities that intuitively make some a priori ‘inefficient’ paths –e.g. long ones– to scale up in a pre-defined efficiency ranking (that would indeed be the case of path P_2 connecting nodes i and j in Fig. 1). Now, in practice both WS and BA mechanisms can have heterogeneous effects on this re-ranking, depending on the particularities of the starting and ending nodes i and j (see SI section S3 for an in-depth microscopic analysis on the effect of these local mechanisms on ξ_{ij} and $\mathbb{L}_{\mathbf{p}(i \rightarrow j)}$). We first start by quantifying how these mechanisms generate a richness of possible trajectories connecting any pair of nodes i and j . The probability that a randomly intercepted trajectory indeed corresponds to one connecting i and j is

$$q_{ij} = \frac{G_{ij}}{\sum_{k < l} G_{kl}}. \quad (7)$$

Then the heterogeneity in the different number of choices for the trajectory of a particle, *i.e.* the trajectory richness of the network is given by the entropy

$$S(\mathbf{q}) = -\frac{1}{2} \sum_{i < j} q_{ij} \ln q_{ij}, \quad (8)$$

that we call the communicability entropy. From an information-theoretic perspective, this entropy is a measure of the ignorance we have on who is the sender node and receiver node, when intercepting a message navigating the network. Since $0 \leq S(\mathbf{q}) \leq \ln(n(n-1)/2)$, the upper bound only reached when the set of probabilities \mathbf{q} are uniform, we define a normalized version $\hat{S}(\mathbf{q}) := S(\mathbf{q})/\ln(n(n-1)/2)$.

Let us now analyze how $\hat{S}(\mathbf{q})$ behaves in our two reference frameworks. Intuitively, for a fixed mean degree $\langle k \rangle$, $\hat{S}(\mathbf{q})$ will increase in the WS model as p increases, since rewiring increases trajectory richness. Likewise, in a BA model one can vary the network's mean degree: for very small $\langle k \rangle$ the resulting BA network is almost tree-like, with no potential bypasses and thus low trajectory richness, whereas when we allow $\langle k \rangle$ to increase, additional routes are formed thus increasing the trajectory richness, hence $\hat{S}(\mathbf{q})$ should also increase. Figures 2.a-b (red axis) confirm our intuitive arguments. In particular, in Fig. 2.a we observe that entropy grows rather quickly in a WS model for small rewiring probability $0 < p \leq 0.4$, reaching a steady maximum afterwards. The impact of rewiring is notably stronger for small p , and this effect is emphasized further for SW networks of increasing $\langle k \rangle$. This behavior is easy to understand: in the small p region there are few shortcuts and each new one makes a difference. On the contrary, for large values of p the entropy saturates very quickly to $\hat{S}(\mathbf{q}) \simeq 1$, i.e. the addition of more shortcuts does not make much of a difference beyond a certain p (see below for further analysis on the influence of the average degree). Figure 2.b reveals a similar behavior of $\hat{S}(\mathbf{q})$ for the BA model as the mean degree $\langle k \rangle$ increases (within the sparse regime for the BA preferential attachment mechanism to hold, see below), reaching full trajectory richness very quickly after a sudden increase in the region of small $\langle k \rangle$ values. In short, rewiring an ordered structure and increasing the link density of an heterogeneous network quickly (nonlinearly) boosts the trajectory richness, and thus the amount of potential bypasses to any specific shortest path connecting any pair of nodes.

We now need to quantify when some of these new routes actually may become consolidated bypasses to shortest paths, like the situation illustrated in Fig. 1, where a particle traveling between two nodes i and j “might prefer” to use P_2 , although being longer (in terms of number of edges to be traversed) than the shortest path P_1 .

Bypass consolidation and associated navigability gain

To evaluate the impact of potential bypasses on the actual navigability, we use Eq. (5) and consider that, for any pair of nodes i and j , the SRP between i and j is a consolidated bypass to the shortest path(s) if the effective length of the SRP is smaller than the effective length of the (potentially many) SPs (i.e. $\mathbb{L}_{SRP}(i, j) < \mathbb{L}_{SP}(i, j)$ for all SPs connecting i and j). Interestingly, this criterion results to be equivalent to check that $\ell_{SRP(i,j)} > \ell_{SP(i,j)}$ (see SI S4 for details). Once bypass detection is done, we need to quantify its impact. A measure that quantifies the impact of bypasses on the network's navigability is the *topological length excess*

$\epsilon_{(i,j)}$

$$\epsilon_{(i,j)} = \left(1 - \frac{\ell_{SP(i,j)}}{\ell_{SRP(i,j)}} \right) \cdot 100, \quad (9)$$

which indicates that, for a particle traveling between two arbitrary nodes i and j , choosing the consolidated bypass SRP over the SP, while beneficial according to the (hidden) network geometry, leads to an *apparent* excess of $\epsilon_{(i,j)}\%$ from the topological distance travelled via the shortest path. It turns out that Eq.25 also quantifies the effective distance per link and the resulting gain of using SRP over SP (see SI S4 for a full derivation of these metrics and their interpretation). To extract a global metric for the whole network, we just average $\epsilon_{(i,j)}$ over all pairs of nodes to define the network navigability gain:

$$\epsilon = \frac{2}{N(N-1)} \sum_{i < j}^N \epsilon_{(i,j)}. \quad (10)$$

An illustration of these metrics in a toy network is given in SI S5. Observe that ϵ quantifies an improvement of a function (network navigability) as a result of an innovation (consolidation of bypasses) and is therefore a quantitative proxy of structural deepening.

We can now quantify bypass consolidation and its associated navigability gain on relation to both WS and BA mechanisms. When we apply this formalism to the evolving SW network we

obtain the results illustrated in panel (a) of Fig. 2 (left axis). We observe that the navigability gain factor ϵ exhibits a clear non-monotonic shape as a function of the rewiring probability p . In fact, our measure detects a maximum for $p \approx 0.15$ at which, on average, traveling through the SRP is much more favorable than doing so through the SP. We call this probability the “good navigational point” (GNP) of the network, p_{GNP} . It is interesting to observe that p_{GNP} is a precise location inside the so-called small-world regime, which is independent of the network mean degree $\langle k \rangle$ (anecdotally, this value appears close to the saturating point of spectral spacing in SW networks [57, 58]).

Now, note that the SW mechanism consolidates bypasses out of a regular-to-random transition, so comparatively speaking the values of ϵ should be typically higher in more structured networks –e.g. in networks with fat-tailed degree distributions like the BA model– where the presence of hubs makes the existence of bypasses even more necessary. This hypothesis is confirmed in Fig.2.b (right axis), in which ϵ reaches roughly values one order of magnitude larger in the BA model than those found in a comparable WS model. In this case we observe again non-monotonic behavior of ϵ with $\langle k \rangle$, displaying a maximum close to $\langle k \rangle \approx 11$, i.e. the BA model also has a good navigational point when mean degree is $\langle k \rangle_{\text{GNP}} \approx 11$, where bypassing shortest paths that include hubs is maximally relevant.

To further analyse the impact of bypasses, we now compare the values of ϵ obtained in a BA model ($n = 250$ nodes and mean degree $\langle k \rangle$) against (i) those obtained for an Erdős-Renyi (ER) graph with the same n and $\langle k \rangle$ –this latter being a model with the same number of edges but with a homogeneous (Poisson) degree distribution and thus virtually lacking any hubs–, and (ii) those of a WS model with the same n and same $\langle k \rangle$, and poised at $p = p_{\text{GNP}}$. Results are shown in Panel (c) of Fig.2 and certify that, in the sparse regime ($\langle k \rangle < 35$), ϵ is substantially larger in

BA than both ER and SW, i.e. the gain supported by bypasses is considerably more important in heterogeneous networks, as expected [59]. When comparing the behavior of ϵ in ER vs SW networks (both in principle lacking substantial hubs), we observe an interesting effect: for a range of small mean degrees $\langle k \rangle < 11$, SW networks benefit more from bypasses than ER ones. The opposite is true for an intermediate $11 < \langle k \rangle < 30$, and the effect is again changed for very large mean degrees $\langle k \rangle > 30$. This nontrivial behavior can be explained by comparing the degree distributions of both ER networks and SW networks at p_{GNP} and by realizing the (often overlooked) fact that the degree distribution (in particular, the skewness and kurtosis) of a SW network poised at a fixed p undergoes different shapes as $\langle k \rangle$ increases (see SI section S8 for details). Incidentally, this can also explain why $\hat{S}(\mathbf{q})$ initial increase in SW networks is sharper for larger $\langle k \rangle$ (see SI).

In summary, the effect of bypasses is maximised for SW networks at the Good Navigational Point $p_{\text{GNP}} \approx 0.15$, and within that point, this effect appears to be monotonically boosted when these SW networks increase their degree heterogeneity, i.e. increasing $\langle k \rangle$. ER networks have bypassing properties as long as they show degree heterogeneities, and to a small extent (Poisson distribution) this is the case. Such effect is then maximal around $\langle k \rangle \approx 20$ (the fact that bypasses have a non-monotonic effect also within ER networks can again be explained in terms of the skewness degree distribution, see SI). Finally, in BA networks, bypassing effects are substantially larger due to higher degree heterogeneities, as expected.

To close this analysis, one can ask about the theoretical upper bound on ϵ . Heuristically, the effect of bypasses would be fully maximized in a situation where we add to a given (connected) network a new node that is linked to every other node. Such new node would be a ‘super-hub’ that makes the network have shortest paths of length ≤ 2 for all pairs of nodes. In this extreme situation, many of the shortest paths will be systematically bypassed, and ϵ would explode (see

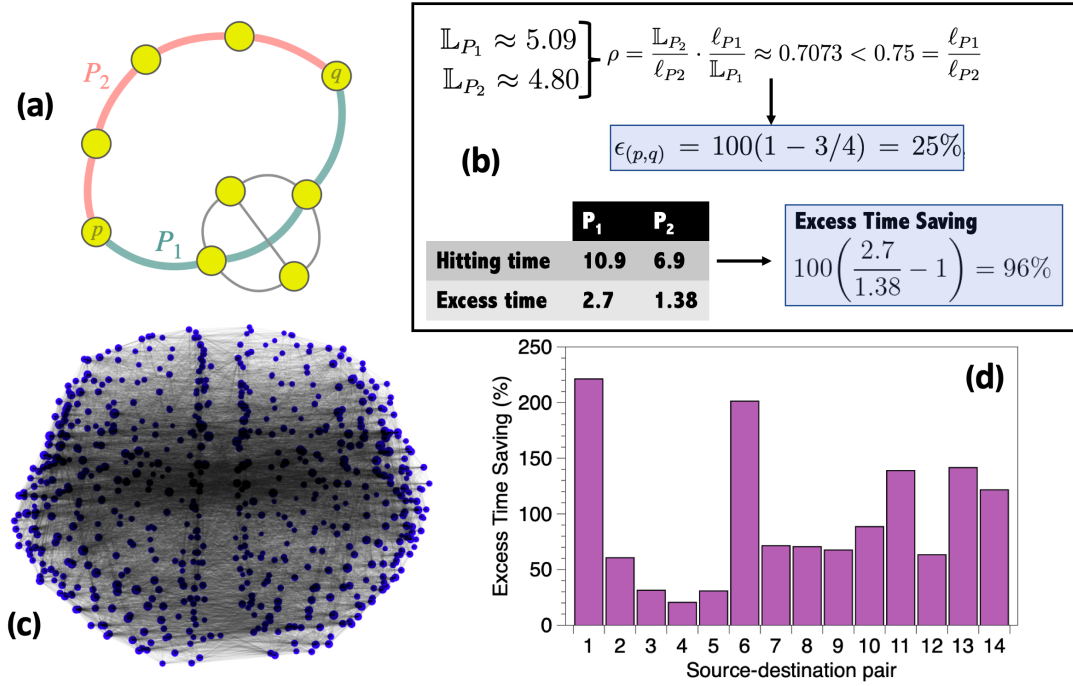


Figure 3: (a) Toy network with a concrete source-destination pair (p, q) which can be navigated via paths P_1 and P_2 . (b) Computation of the different metrics certify that P_2 is a bypass of the shortest path P_1 , and the navigability gain associated to this pair is 25% (a lower bound of the actual gain, see SI S5). Random walk trajectories starting at p and eventually hitting q can be classified as P_1 -like or P_2 -like, depending on their specific trajectories (SI S6). The hitting time and excess time of the P_1 class is larger than for P_2 , meaning that random-walk navigability is enhanced in the P_2 (that is, the SRP) class. The excess time saving is a diffusion-proxy of the navigability gain (see SI S6). (c) Coactivation brain network. (d) Excess time saving for several source-destination pairs in the brain network, finding that SRP enhances navigability in all cases.

SI S9 for details). Now, is this just a theoretical scenario? It turns out that this situation can take place in an extreme version of the BA model in a finite graph, where $\langle k \rangle$ is large enough (compared to the initial seed) so that new nodes entering systematically connect to a large portion of the network, leading to so-called ultra-short graphs [60]. This explosion is reported in Panel (f) of Fig.2. Evidently, in this case there is no preferential attachment anymore, so in some sense the rationale behind the BA model breaks down in this dense regime³.

³In the dense regime $\langle k \rangle > 35$ the calculations of ϵ need to be taken with caution as numerical rounding effects might become important when computing $\exp(A)$.

Effect on Dynamics

As already anticipated, our theory is purely structural and therefore dynamically-agnostic, and speaks of the effect of network geometrization on the formation of shortest paths in the geometrized network –the SRPs– which are different from the shortest paths of the original, un-geometrized network. Our contention is that these emergent bypasses have an effect on the network’s navigability, and here we provide a first validation of this hypothesis by considering source-destination random walk trajectories navigating a network. Each of these random walk trajectories is then classified as SRP-like or SP-like depending on the specific sequence of nodes the walker is visiting (see SI S6 for details). One can subsequently compare the SRP class and the SP class by computing a number of quantities, such as the average hitting time in each class, or the excess time (i.e., for each class, how much more time than the time spent by a ballistic walker it takes to reach the destination), which yield dynamical proxies for the effective length or the associated navigability gain defined above (see SI S6). Results for both a synthetic small network and for a large, real network (a coactivation brain network, see below) are shown in Fig.3, and confirm our hypothesis that particles are more prone to ‘get lost’ (and thus spend a significantly longer time) navigating through a SP-like path compared to a SRP-like one. In other words, the presence of SRPs enhances navigability for diffusion-like dynamics (additional details and analysis are provided in SI S6). At the same time, this finding further confirms that bypasses induce structural deepening by increasing the efficiency of network navigability.

We have also made some preliminary progress on analysing how bypasses impact other network functions by considering two additional dynamical processes running on a network: synchronization and epidemic spreading. Results (fully detailed in SI section S7) suggest that the prototypical dynamical fingerprints in each case (i.e. eigenratio of the Laplacian matrix for synchronization, and epidemic threshold for epidemic spreading) are affected by bypass con-

Network	$\hat{S}(q)$	ϵ (%)	p^*	ϵ/ϵ_{BA}
Human brain (functional, task-driven)	0.9234	51.71	0.30	0.78
Collaboration CoGe	0.7776	41.50	0.21	0.93
Collaboration QcGr	0.4598	38.39	0.15	0.79
Human brain (anatomical)	0.925 ± 0.022	36.21 ± 1.52	0.23 ± 0.01	0.86 ± 0.04
<i>C. elegans</i> neurons	0.9312	31.69	0.34	0.87
USA airports 1997	0.8501	28.60	0.27	0.76
Internet AS 1997	0.8891	25.49	~ 1	0.52
Yeast PPI	0.8344	25.50	0.24	0.55
Drugs users	0.7794	21.18	0.10	0.57
Software	0.8308 ± 0.0263	21.11 ± 12.10	$\sim 1^\dagger$	0.58
Human brain (functional, resting-state)	0.758 ± 0.054	20.81 ± 1.42	0.17 ± 0.02	0.49 ± 0.05
Roget thesaurus	0.9215	19.18	0.35	0.43
Transcription yeast	0.8128	12.26	~ 1	0.38
Food webs	0.9498 ± 0.0208	9.94 ± 7.13	**	0.64***
electronic circuits	0.8202 ± 0.0260	3.456 ± 2.561	~ 1	0.12
Termite mounds	0.5707 ± 0.0331	3.100 ± 2.12	~ 1	0.11
Power grid	0.6348	2.61	~ 1	0.05

Table 1: Summary of metrics for empirical networks, depicting the communicability entropy $\hat{S}(q)$, the navigability gain ϵ , the optimal rewiring probability p^* and the navigability ratio ϵ/ϵ_{BA} (see the text) across 177 different empirical networks (for many of them, we offer averages, see S10 for details), where: *Human brain (anatomical)* provides the averaged results across 70 anatomical networks (using the same parcellation), *Human brain (functional, resting-state)* provides the averaged results across 70 functional networks (using the same parcellation as the anatomical networks), *Software* provides the averaged results across the networks MySQL, XMMS, Abi, Digital and VTK; *Food webs* is the average of 15 food webs (see SI S11.3 for disaggregation); *Electronic circuits* is the average of three electronic circuits; *Termite mounds* is the average of three termite mounds. \dagger Except MySQL which has $p^* \approx 0.29$. **Three types of behaviors: (i) $p^* \approx 1$ for 8 food webs; (ii) $0.43 \leq p^* \leq 0.45$ for El Verde, Shelf, Ythan1 and Ythan2; (iii) $0.03 \leq p^* \leq 0.14$ for Bridge Brooks, Coachella, Little Rock. *** See SI section S11 for disaggregated data and additional details.

solidation, and in particular, qualitative dynamical changes occur in both types of dynamics close to p_{GNP} .

Empirical networks

To round off, we have considered a total of 177 empirical networks of different nature, including social (4 collaboration networks of different nature, 3 termite mounds), biological (Human

brain –70 anatomical, 70 functional at resting-state, one functional at task-driven (extracted and averaged from a meta-analysis of 1600 works)–, neural network of *C. elegans*, a protein-protein interaction, a transcription yeast, 15 food webs) and technological ones (air transportation, Internet, 3 electronic circuits, power grid, 5 software networks), see SI section S11.1 for details and full references. Results on several metrics are summarised in table 1 and some scatter-plots are visualised in Fig.4.

The first two columns of this table report the normalized communicability entropy $\hat{S}(q)$ and navigability gain ϵ . Interestingly, all of them appear to be entropic enough for potential bypasses to have been formed, as values of $\hat{S}(q)$ are in the region where our analysis on synthetic models show consolidated bypasses⁴. We indeed find that essentially all real-world networks harbor consolidated bypasses ($\epsilon > 0$), albeit with different impacts, what allows us to rank them accordingly. At the top of the ranking, the net gain induced by consolidated bypasses reaches over 50% for (task-driven) functional brain network, followed by many other self-organised networks (collaboration networks, *C. elegans*, etc). It is interesting to see that the navigability gain substantially drops for functional brain networks when passing from task-driven activation to resting-state. This might be suggesting the possibility that navigability gain in functional brain networks might be task-related, something that deserves further research. Finding anatomic networks somehow interpolating task-driven and resting-state functional networks is reasonable, given that resting-state function in adults is usually thought to be restricted to a brain module and that the specific task-driven network we analyse is the outcome of a meta-analysis of over 1,600 works considering different tasks –and thus, in principle, multiple brain modules–. These hypothesis await confirmation and, in any case, further research is needed to elucidate the relation of the topology-induced bypasses studied here with specific cognitive aspects.

⁴Note, however, that a finer analysis is needed as e.g. we have observed in the SW analysis that reaching the GNP is density-dependent, i.e. the communicability entropy saturates quicker as p increases for networks with larger mean degree.

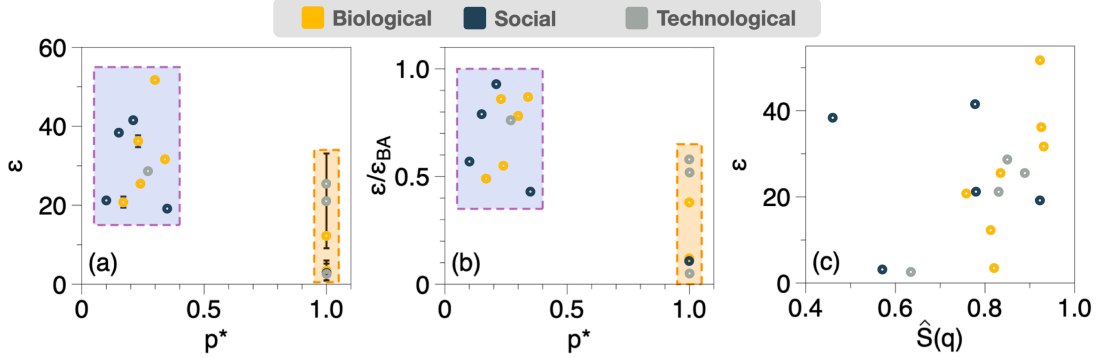


Figure 4: Some scatter plots of the metrics reported in table 1 for empirical networks. (a) Net navigability gain ϵ vs p^* , revealing the emergence of two well-defined groups of networks. (b) Navigability ratio ϵ/ϵ_{BA} vs p^* , finding the same clustering as in panel (a). (c) ϵ vs the normalized communicability entropy $\hat{S}(q)$, where no clear clustering emerges.

At the bottom of the list in table 1 we find some designed networks, such as electronic circuits or the power grid, the latter having only a discrete 2.6% navigability gain. This can be indicative that the power grid, while having hubs to some extent [4, 62], has not evolved according to mechanisms such as WS or BA, is not self-organised and as a consequence does not hold the necessary preemptive structural bypasses to avoid systemic failures, as we have seen during blackouts [63]. Note at this point that the navigability gain ϵ does not trivially correlate with more standard network metrics, such as network density (linear regression of the scatter plot offers a $R^2 = 0.12$), mean degree ($R^2 = 0.09$), average path length ($R^2 = 0.01$) or average clustering ($R^2 = 0.006$), see SI 11.4 for details.

Now, to which extent the observed bypasses are indeed of the SW-type (i.e. bypassing shortest paths consistently generated via a WS-like mechanism), and in such case, how close empirical networks are to their theoretical Good Navigational Point? While this question is difficult to answer, the metric p^* reported in the third column of table 1 (see also Fig.4) provides a first step. Operationally, for a given empirical network \mathcal{G} with n nodes and mean degree $\langle k \rangle$, we estimate

the closest purely SW-generated network $\mathcal{G}'(p)$ (with the same $(n, \langle k \rangle)$). This is achieved by minimizing the spectral dissimilarity distance $\mathcal{D}(\mathcal{G}, \mathcal{G}') = \sqrt{\sum_{j=1}^n (\lambda_j(\mathcal{G}) - \lambda_j(\mathcal{G}'))^2}$, where $\lambda_j(\mathcal{G})$ is the j -th eigenvalue of the adjacency matrix of network \mathcal{G} and minimization is over p , i.e. $p^* = \operatorname{argmin}_p [\mathcal{D}(\mathcal{G}, \mathcal{G}'(p))]$ ⁵. This metric indicates that networks can be typically clustered in two types: one (which includes all human brain networks, the neural network of *C.elegans*, the protein-protein interaction network, collaboration networks, Roget network and the US air network) where $\mathcal{D}(\mathcal{G}, \mathcal{G}'(p))$ has a non-monotonic shape with a minimum $p^* \in [0.15, 0.35]$ –i.e., close but not exactly at the Good Navigational Point–, and another cluster of networks (including electronic circuits, Internet AS97, software networks of termite mounds) where $\mathcal{D}(\mathcal{G}, \mathcal{G}'(p))$ is monotonically decreasing and thus $p^* = 1$ (see SI S11.2 for further details and analysis). The former class thus tends to harbor bypasses of the SW-type –avoiding shortcuts– and its network formation includes at least partially some SW ingredient while the second one tends to have a structure which cannot be well-explained only by SW mechanisms (this doesn't mean, however, that such network is random). Incidentally, no clear function-related clustering emerges.

The fourth column of table 1 finally depicts ϵ/ϵ_{BA} –where ϵ_{BA} is the navigability gain of a BA network with the same number of nodes n and mean degree $\langle k \rangle$ of the real network–, and quantifies whether the observed network bypasses are effectively bypassing hubs. This metric highlights a group of networks where hubs are relevant (i.e. $\epsilon/\epsilon_{BA} \sim 1$) and another group of networks where consolidated bypasses are either not necessarily bypassing hubs, or they are networks that even if having hubs, have not been designed to harbor bypasses and thus do not abide to a BA-like mechanism, so ϵ/ϵ_{BA} closer to zero (see SI S11.3 for further discussion).

⁵Note that this analysis is not designed to find which real-world networks can be classified as small-world. It just assumes they all have such ingredient in their network formation, and evaluate, setting that prior as the sole generating mechanism, what would then be the value of the rewiring probability, so as to establish whether the bypass amount is close or not to the GNP. For those networks whose p^* is found to be close to the GNP, this is partial evidence that such network harbors bypasses of the SW-type.

3 Discussion

The journey of network complexification is supported by basic mechanisms including the celebrated WS and BA, among others. As the network evolves accordingly, we have shown that it naturally increases its communicability entropy $S(\mathbf{q})$ and, in so doing, it allows for new navigational routes to be built, entropically providing bypass ‘candidates’ to the network. Our theory allows to detect when some of these new routes consolidate their bypassing property by subsequently getting to be more favorable than the corresponding shortest paths connecting the same pairs of nodes, and we show that consolidation takes place in both WS and BA models. Interestingly, we find that the role of bypasses is maximised in a small parameter region –which we call the network’s Good Navigational Point–, located in a point inside the Small-World regime and for a specific mean degree in the BA model. These findings suggest that the navigation gain offered by the network bypasses is indeed reflecting a form of structural deepening, thus putting the onset of complexity in networks into a solid quantitative footing.

We have certified that bypasses induce clear navigation gain for particles undergoing diffusion-like dynamics and also play an effect on other network functions, including harboring synchronization and epidemic spreading. We have then shown that many empirical networks considered complex, including brain networks, indeed have Good Navigational Point properties, while those that are not catalogued as self-organised but have been designed tend to not include bypasses in their design, with well-known unfortunate consequences [63].

In hindsight, our results could provide a theoretical and mechanistic support for the role of bypasses in e.g. physiological systems, –where plasticity is of utmost importance [24]–. First, network bypasses naturally relate to the existence of the so-called “collateral circulation”: a

system of specialized endogenous bypass vessels present in most tissues providing protection against ischemic injury caused by ischemic stroke, coronary atherosclerosis, peripheral artery disease and other conditions and diseases [35]. Second, in brain networks, there is nowadays enough observational evidence which supports that these are SW in the Watts-Strogatz sense [25] and possess hubs which create skewness of their degree distributions [26]. At the same time, recent experiments [27] suggest that propagating signals in the brain using hubs as part of the navigation path might have a large energetic cost, triggering research on non-geodesic information propagation [27, 28, 29]. Our work indeed supports the concept of non-geodesic navigability (via network bypasses), and reconciles this with the reported network structure. In this context, note that [30] proposed considering networks of neurons as evolving and growing connections in a distributed fashion (via mechanisms different than SW or BA), such that shortest path minimization and robustness maximization (which in general implied to avoid the creation of hubs) was performed at the same time. Note, however, that brain navigation is not likely to occur always geodesically [27, 28, 29] (this also would imply that individual neurons perform global optimization and have access to the whole brain structure). The logical conclusion is that the seminal findings in [30] imply that the creation of shortest paths should be accompanied by the proliferation of additional structure that plays a role of structural deepening, in good agreement with our theory.

Third, in another recent work [64] it has been shown that brain function appears to be robust against damage by re-adapting and re-purposing non-damaged links, something that can be interpreted to the brain's ability to re-compute SRPs and thus re-rank bypasses after network damage. All in all, elucidating the impact of our findings in the context of neuroscience is an exciting avenue for future work.

An aspect not explored in this paper but also of major interest is the implications of our theory to congestion or jamming phenomena in networks, and to which extent our proposed measures of topological length excess and navigability gain could anticipate congestion in e.g. transportation and urban systems. First, we should disclose that conceptually similar problems have been theorized in the mathematics literature, where some authors have studied the so-called “resistance distance” in networks [31] –where some unit resistances are placed at every edge in a network– in the context of congestion [32, 33]. Now, while an interesting mathematical concept, this latter distance analytically converges, for large graphs and in high dimensions, to an expression that does not take into account the structure of the graph [34] (i.e. it only depends on the degrees of the source and destination nodes) and thus unfortunately turns useless in real-world scenarios⁶. Second, recent empirical evidence in urban science indeed suggests that, at rush hours, in different cities worldwide paths which can be identified as SRPs are supporting more traffic than SPs [67], i.e. they become systematically preferred routes. This constitutes preliminary support in favor of the relevance of SRPs for navigation strategies in networks subject to jamming, and further research is deserved. For instance, we speculate that this strategy can be further refined by, instead of systematically selecting only the SRP as the preferred route, ranking each of the paths connecting any two locations via the computation of its associated topological length excess and rerouting traffic accordingly when needed.

Other important open questions for further research include understanding the role played by network bypasses and their relation to structural deepening in other mechanistic growth models (e.g. assortative/dissortative mixing, triadic closure, etc), and the extension of our theory to weighted (see a preliminary discussion on this topic in SI S10), temporal and higher-order networks [65, 66].

⁶Anecdotally, it is easy to see that such resistance distance is already unable to capture the nuanced navigability properties of paths P1 and P2 in the toy network presented in Fig.3 (revealed by the hitting times analysis) and that in turn our theory correctly predicts.

Finally, while network bypass emergence appears to be contingent on the growth mechanism –and thus appears to be a byproduct of it–, bypass consolidation (structural deepening) is the effect which probably makes those growth mechanisms to be sustainable in the first place. Simply put, we argue, bypasses sustain complexity.

Acknowledgments The authors thank Olaf Sporns, Yasser Aleman-Gomez and Yasser Iturria-Medina for assistance with the data and analysis of brain networks, Adrian Garcia-Candel for help formatting Fig1, and referees for insightful comments. EE acknowledges funding from project OLGRA (PID2019-107603GB-I00) funded by Spanish Ministry of Science and Innovation. J.G.-G. acknowledges financial support from the Departamento de Industria e Innovación del Gobierno de Aragón y Fondo Social Europeo (FENOL group grant E36-23R) and from project TEAMS (PID2020-113582GB-I00) funded by the Spanish Ministry of Science and Innovation. L.L. acknowledges funding from project DYNDEEP (EUR2021-122007) and project MISLAND (PID2020-114324GB-C22), both projects funded by Spanish Ministry of Science and Innovation. This work has also been partially supported by the Maria de Maeztu project CEX2021-001164-M funded by the MCIN/AEI/10.13039/501100011033.

Contributions EE and LL designed the research and EE performed the computational and analytical calculations. LL and JGG contributed additional computational analysis. EE and LL wrote the first draft of the paper. All authors discussed results and revised the paper.

Competing financial interests The authors declare no competing financial interests.

Additional information Correspondence and requests for materials should be addressed to Ernesto Estrada (estrada@ifisc.uib-csic.es).

Supplementary information

S1. Network Communicability $G_{ij}(\beta)$

S1.1 Network communicability across the disciplines. The communicability function emerges in a variety of physical scenarios: it was proved in [38] that $G_{ij}(\beta)$ corresponds to the thermal Green's function of a network of coupled quantum harmonic oscillators where β represents the inverse temperature of the thermal bath in which the network is submerged. The self-communicability $G_{ii}(\beta)$ also appears in the definition of the probability of finding a network, represented by a tight-binding Hamiltonian, in a state with energy $E_j = -\lambda_j$ when the system has inverse temperature equal to β [69]. More recently, Lee et al. [40] found that the communicability function appears in the solution of a linearised upper bound to the susceptible-infected (SI) model when certain initial conditions are imposed to the epidemic dynamics. Similar results were extended by Bartesaghi and Estrada [41] for the SIS model. Finally, the communicability emerges as the solution of a linear autonomous system, which is a modification of the Kuramoto model, when the internal frequency of the oscillators is zero [42]. Nowadays communicability is used for the analysis of the structure and dynamics on brain networks, granular material, infrastructural systems, social networks, biological patterns, genomic and proteomic systems, among others (see references in the main article).

S1.2 Derivation of the communicability function in a concrete setting. For illustration, here we present the derivation of the communicability function and subsequent operators in case for the dynamics of a particle hopping on a network following the tight-binding Hamiltonian:

$$\mathcal{H} := \sum_{v=1}^n \varepsilon_v |v\rangle \langle v| + \sum_{v \neq w} A_{vw} t_{mn} |w\rangle \langle v|, \quad (11)$$

where $\mathbf{A} = \{A_{vw}\}_{v,w=1}^n$ is the network's adjacency matrix, and t_{mn} is the hopping parameter, which represents the energy that facilitates the hopping of a particle from v to w . If this pa-

rameters tends to zero the particles cannot move from one site to another (an isolated or trivial graph). If we turn on the parameter, the particles can hop from one site to the other. Here we fix it as $t_{mn} = 1$ for the sake of simplicity. The eigenstates of the Hamiltonian are represented in the Dirac bra-kets notation as usual.

In the initial value representation, the probability amplitude for a transition from state (node) v at time zero to state (node) w at time t is given by $G_{vw}(t) = \langle \psi_w | e^{-it\mathcal{H}/\hbar} | \psi_v \rangle$. Applying a Wick rotation $t \rightarrow i\beta\hbar$, the real-time propagator $e^{-it\mathcal{H}/\hbar}$ is mapped into the thermal propagator $e^{-\beta\mathcal{H}}$, where β is the inverse temperature of a thermal bath in which the network is submerged into. Setting $\varepsilon_v = 0$ for every node and $t_{mn} = -1$ for every pair of nodes, as it is done in the tight-binding model, we identify $\mathcal{H} = -\mathbf{A}$ and the propagator reduces to the communicability function $G(\beta) = e^{\beta\mathbf{A}}$.

Then, for a particle located at the node v at time zero, the difference:

$$R_{vw}(\beta) := \langle \psi_v | e^{\beta\mathbf{A}} | \psi_v \rangle - \langle \psi_w | e^{\beta\mathbf{A}} | \psi_v \rangle, \quad (12)$$

accounts for the opposition offered by the network to the displacement of the particle to the node w at inverse temperature β . The smallest the values of $R_{vw}(\beta)$ the highest the probability that the particle does not get trapped at the origin and can propagate to node w . One can symmetrize this quantity to define the following operator:

$$\xi_{vw}^2(\beta) := R_{vw}(\beta) + R_{wv}(\beta) = \langle \psi_v - \psi_w | e^{\beta\mathbf{A}} | \psi_v - \psi_w \rangle. \quad (13)$$

Mathematically, one can prove that ξ_{vw} is an Euclidean distance between the corresponding nodes (see SI below). Conceptually, ξ_{vw} is indeed a measure of the network opposition to the flow between v and w . As a matter of fact, and as we will show below, ξ_{vw} is indeed formally

equivalent to the so-called effective resistance found between a pair of nodes v and w in an electric circuit, which is expressed as $\langle \psi_v - \psi_w | L^* | \psi_v - \psi_w \rangle$, where L^* is the Moore-Penrose pseudoinverse of the circuit's Laplacian matrix. By analogy, we call ξ_{vw} the communicability resistance between nodes v and w in the network.

S2 ξ_{vw} is an Euclidean distance

Theorem 1. *Let $\xi_{vw}^2 := (e^A)_{vv} + (e^A)_{ww} - 2(e^A)_{vw}$, where A is the adjacency matrix of a graph. Then, ξ_{vw} is an Euclidean distance between the nodes v and w .*

Proof. Let $A = U\Lambda U^T$ where the j th column of U is ψ_j and $\Lambda = \text{diag}(\lambda_j)$. Then,

$$\begin{aligned} \xi_{vw}^2 &= \sum_{j=1}^n e^{\lambda_j} \psi_{jv}^2 + \sum_{j=1}^n e^{\lambda_j} \psi_{jw}^2 - 2 \sum_{j=1}^n e^{\lambda_j} \psi_{jv} \psi_{jw} \\ &= \sum_{j=1}^n e^{\lambda_j} (\psi_{jv} - \psi_{jw})^2 \end{aligned} \quad (14)$$

Let us define φ_v to be the v th column of U^T , such that we can write

$$\xi_{vw}^2 = (\varphi_v - \varphi_w)^T e^A (\varphi_v - \varphi_w), \quad (15)$$

then, because e^A is positive definite we can write

$$\xi_{vw}^2 = (e^{A/2} \varphi_v - e^{A/2} \varphi_w)^T (e^{A/2} \varphi_v - e^{A/2} \varphi_w). \quad (16)$$

Let us designate $x_v := e^{A/2} \varphi_v$, such that we have

$$\begin{aligned} \xi_{vw}^2 &= (x_v - x_w)^T (x_v - x_w) \\ &= \|x_v - x_w\|^2, \end{aligned} \quad (17)$$

which means that $\xi_{vw} = \sqrt{\|x_v - x_w\|^2}$ is a Euclidean distance between v and w . Therefore, x_v and x_w are the coordinates of the nodes v and w in such Euclidean space. \square

S3 How communicability and effective distance change with network rewiring: a microscopic analysis

Let us consider the effective length of a path P between the nodes i and j as

$$\mathbb{L}_{P(i,j)} = \sum_{e_k \in P} \xi_{e_k} = \left(\sum_{e_k \in P} \xi_{e_k}^2 + 2 \sum_{e_k \neq e_l} \xi_{e_k} \xi_{e_l} \right)^{1/2}, \quad (18)$$

where e_k is an edge in the path P , where the second equality is used for convenience and simply uses the fact that $a + b = \sqrt{a^2 + b^2 + 2ab}$ (which can always be made since ξ is a distance and thus non-negative).

The first term inside the square root is given by

$$\sum_{e_k \in P} \xi_{e_k}^2 = G_{ii} + 2 \sum_{s \in P} G_{ss} + G_{jj} - 2 \sum_{(r,t) \in e_k \in P} G_{rt}, \quad (19)$$

where i and j are the endpoints of the path P , s are intermediate nodes in the path and (r, t) are every adjacent pairs of nodes belonging to the corresponding path.

Then, in order to drop the effective length of the path P relative to another path connecting the same pair of nodes i and j –for instance, relative to the SP– we can act in any of the following two cases:

1. Dropping $\sum_{s \in P} G_{ss}$ to any node in P relative to the similar sum in the reference path. This can be done by dropping the number of small subgraphs in which nodes in the path P participates. For instance, we can delete edges or triangles attached to any node in the path P .
2. Increasing $\sum_{(r,t) \in e_k \in P} G_{rt}$ to any pair of nodes forming an edge in P relative to the similar sum in the reference path. This can be done by increasing the communication capacity of pairs of nodes in the path P . For instance, by dropping the length of the cycles in which the two nodes are involved or by increasing the number of paths between pairs of nodes in the path P .

Using only this contribution we can see how the two growing mechanisms studied in this paper may affect these two cases. The rewiring process of the WS mechanism can influence the two cases analyzed in the following way. The rewiring may remove edges attached to nodes which are in the path under consideration (Case 1), at the same time such rewires can create shortcuts that increases the communicability between alternative paths (Case 2). Additionally, the rewiring may attach edges to pairs of nodes in the SP and also can drop the communicability between others which are in the SP. In the case of the BA model, it must be remarked that the addition of a node connected to the nodes of the network will not drop the self-communicability of any node (Case 1 is not possible). Therefore, such mechanism can drop the effective length of a path by increasing the communicability between pairs of nodes in the path or by increasing the self-communicability of nodes in the SP.

The second term in Eq.18 represents the interaction between pair of edges in the graph, where each individual term can be written as:

$$\xi_{e_k} \xi_{e_l} = \left(\sum_{s \in e_k, r \in e_l} G_{ss} G_{rr} - 2 \sum_{s \in e_k, (r,t) \in e_l} G_{ss} G_{rt} + 2 \sum_{(p,q) \in e_k, (r,t) \in e_l} G_{pq} G_{rt} \right)^{1/2}, \quad (20)$$

where the first term is the sum of the product of self-communicabilities of nodes s and r , where the two nodes are always in different edges, the second term is the product of the self-communicability of a node in one edge with the communicability between a pair of nodes in another edge, and the last term is the product of the communicability between two nodes in one edge and the one between the two nodes in another. This second term in the expression of $\mathbb{L}_P(i,j)$ indeed introduces nonlinearities in the influence of the self-communicability and internode communicability on the change of the length of a path after a given transformation. For instance, we have seen that dropping $\sum_{s \in P} G_{ss}$ will make the path less resistant, according to the first term of the expression. This dropping also contributes to drop $\sum_{s \in e_k, r \in e_l} G_{ss} G_{rr}$, which makes the path less resistant, but it contributes to increase the effective length of the path P via

the term $2 \sum_{s \in e_k, (r,t) \in e_l} G_{ss} G_{rt}$. A similar analysis is possible with the communicability G_{rt} , whose increment drops the term $2 \sum_{s \in e_k, (r,t) \in e_l} G_{ss} G_{rt}$, but increases $2 \sum_{(p,q) \in e_k, (r,t) \in e_l} G_{pq} G_{rt}$. As a consequence of the different types of contributions emerging in both terms, there will be a trade off between the self-communicability and the internode communicability, such that changing them in the appropriate direction will drop the effective length of the path P relative to the SP only up to certain point after which the effective length will increase.

S4 Derivation of the bypass consolidation criterion and measures of impact of bypass consolidation in network navigability

S4.1 Bypass consolidation criterion Take two arbitrary nodes s and t , and denote $\mathcal{S}_{(s,t)}$ the set of all shortest paths connecting s and t (this set has at least one element, but it might have many more, and that is typically the case when the network is large and the nodes s,t are distant, topologically speaking). Let us denote $\mathcal{P}_{(s,t)}$ the set of potential bypasses. This consists of all paths connecting s and t except the set of shortest paths

$$\mathcal{P}_{(s,t)} = \{\mathbf{p}(s \rightarrow t)\} \setminus \mathcal{S}_{(s,t)}.$$

We say that any given path $\mathbf{p}(s \rightarrow t)$ is a consolidated bypass if

$$\mathbb{L}_{\mathbf{p}(s \rightarrow t)} < \min_{\mathbf{SP}(s,t) \in \mathcal{S}_{(s,t)}} [\mathbb{L}_{\mathbf{SP}(s,t)}]. \quad (21)$$

It is clear that, for a given pair of nodes (s, t) , applying Eq.21 for all elements in $\mathcal{P}_{(s,t)}$ can yield no solutions, one solution, or multiple solutions. To make the quantification simpler, instead of looking for the total number of consolidated bypasses of (s, t) , we only consider a specific path, i.e. the one which has the smallest effective length, i.e. the SRP. In this way, we say that the shortest path(s) are bypassed if

$$\mathbb{L}_{SRP(s,t)} < \min_{\mathbf{SP}(s,t) \in \mathcal{S}_{(s,t)}} [\mathbb{L}_{\mathbf{SP}(s,t)}]. \quad (22)$$

Observe that, by definition of the Shortest Resistive Path, for any shortest path we always have

$$\mathbb{L}_{SRP(s,t)} \leq \mathbb{L}_{SP(s,t)},$$

and at the same time, by definition of the Shortest Path(s), we always have

$$\ell_{SP(s,t)} \leq \ell_{SRP(s,t)}. \quad (23)$$

These two properties imply that if Eq.22 is satisfied, then necessarily we have as a consequence that

$$\ell_{SRP(s,t)} > \ell_{SP(s,t)}. \quad (24)$$

In fact, if $\ell_{SRP(s,t)} > \ell_{SP(s,t)}$ then it follows that $\mathbb{L}_{SRP(s,t)} < \min_{SP(s,t) \in \mathcal{S}(s,t)} [\mathbb{L}_{SP(s,t)}]$ (the other alternative would imply that the SRP is indeed a shortest path and thus not a bypass, resulting in a contradiction). Accordingly, SRP(s, t) is a consolidated bypass if and only if Eq.24 holds. In fact the same criterion holds to assess if any $p(s \rightarrow t)$ is a consolidated bypass, but as previously mentioned we won't be analysing the abundance of bypasses, only whether for a given s, t , one consolidated bypass exists. It is trivial to see that checking the SRT is a sufficient condition, so we focus on the SRT.

S4.2 Quantification of bypass effect Once we have a principled way of assessing if the SRP is a consolidated bypass, we wish to characterize its effect on the navigability of the network. There are two independent aspects one can look at.

First, one can assess how larger is the topological distance of the SRT with respect to the SP, i.e. how small the ratio $\frac{\ell_{SP(s,t)}}{\ell_{SRP(s,t)}} < 1$ is. From this we can define the *topological length excess*

$\epsilon_{(s,t)}$

$$\epsilon_{(s,t)} = \left(1 - \frac{\ell_{SP(s,t)}}{\ell_{SRP(s,t)}} \right) \cdot 100, \quad (25)$$

which indicates that, for a particle traveling between two arbitrary nodes i and j , the choice of consolidated bypass SRP over the SP, while beneficial, leads to an *apparent* excess of $\epsilon_{(s,t)}\%$

from the topological distance travelled via the shortest path. Since Eq.25 is a ratio, then it can be properly averaged across all pairs to construct an average topological length excess

$$\epsilon = \frac{2}{N(N-1)} \sum_{s < t}^N \epsilon_{(s,t)}, \quad (26)$$

that quantifies the average effect of bypasses across all pairs of nodes in terms of the resulting increase in topological length.

Second, we can ask ourselves why would a walker prefer to take a path of, say, topological length $\ell = 9$, than another of, say, topological length $\ell = 3$? Of course this is the case if the first path has smaller effective distance (the walker might diffuse out in the second route, thus getting lost –if the walker was a diffusive one– using that other route, etc), but this information does not seem to be easily interpreted from Eqs.25 and 26. So to some extent knowing that a walker still prefers a path of topological length three times larger gives also rough idea of the underlying (hidden) resistive geometry. Let us explain this: For the sake of argument, let us suppose that we have detected a consolidated bypass SRP with a certain effective length $\mathbb{L}_{SRP} < \mathbb{L}_{SP}$, and consider two hypothetical situations: (1) in the first one we would have $\ell_{SRP(s,t)} \gg \ell_{SP(s,t)}$, and (2) in the second, $\ell_{SRP(s,t)}$ is only marginally larger than $\ell_{SP(s,t)}$. Clearly, in the first situation the walker navigating from s to t choosing SRP would need to traverse a proportionally much larger amount of edges than by choosing the SP than in the second situation. Since, we need to recall, this is utterly beneficial (because SRP is at the end of the day a consolidated bypass of the SP), this necessarily means that not only the effective length of the SRP is *smaller* than the effective length of the SP (true by definition of the consolidated bypass), but furthermore, it means that the ratio between the effective length *per edge* in the SRP and in the SP is notably smaller in the first situation than in the second. In formulas, the average effective length per edge in the SRP and SP are

$$\langle \mathbb{L}_{SRP(s,t)} \rangle = \frac{\mathbb{L}_{SRP(s,t)}}{\ell_{SRP(s,t)}}; \quad \langle \mathbb{L}_{SP(s,t)} \rangle = \frac{\mathbb{L}_{SP(s,t)}}{\ell_{SP(s,t)}}$$

and then the ratio

$$\rho = \frac{\langle \mathbb{L}_{SRP(s,t)} \rangle}{\langle \mathbb{L}_{SP(s,t)} \rangle} \quad (27)$$

quantifies the net benefit (reduction) in effective distance per edge in choosing SRP over SP. ρ is thus the correct measure to compare (and also to average) such benefit for different bypasses. Unfortunately, evaluating Eq.27 is only computationally efficient for small networks, and in general is not scalable (see however next section for a concrete illustration where such computation is performed). This is mainly due to the fact that in a large unweighted network, in general between any two nodes there might be very many shortest paths –all of them with the same topological length but different effective length–. To exhaustively enumerate all these paths is in general a difficult task, and it is thus much easier to compute $\ell_{SP(s,t)}$ than $\mathbb{L}_{SP(s,t)}$. On the other hand, computing $\mathbb{L}_{SRP(s,t)}$ is actually computationally efficient: once the network is geometrized, it effectively converts into a weighted network with real-valued weights, and the shortest path in this geometrized network (which is indeed the SRP of the original network) is almost surely unique, so a Dijkstra’s algorithm finds it without ambiguity, and without the needs to exhaustively enumerate all possible paths, including the very many shortest paths of the original network. Interestingly, by using the properties of SRP and SP we can show that

$$\rho = \frac{\mathbb{L}_{SRP(s,t)} \ell_{SP(s,t)}}{\mathbb{L}_{SP(s,t)} \ell_{SRP(s,t)}} \leq \frac{\ell_{SP(s,t)}}{\ell_{SRP(s,t)}} \leq 1. \quad (28)$$

In words, ρ quantifies how much more beneficial it is –in terms of effective distance travelled per edge– to travels through the SRP than through the SP, and this gain is bounded by $\ell_{SP(s,t)}/\ell_{SRP(s,t)}$. This upper bound is computationally efficient to work out for large networks and in fact, we have already computed it in the bypass consolidation criterion and in Eqs.25 and 26 ! Using this upper bound as a conservative approximation of ρ , it turns out that the *topological length excess* $\epsilon_{(s,t)}$ can now be interpreted as a lower bound of the *effective distance gain per edge* of using SRP over SP, and likewise ϵ is the network’s *average effective distance*

saving in the navigability that bypasses have globally provided.

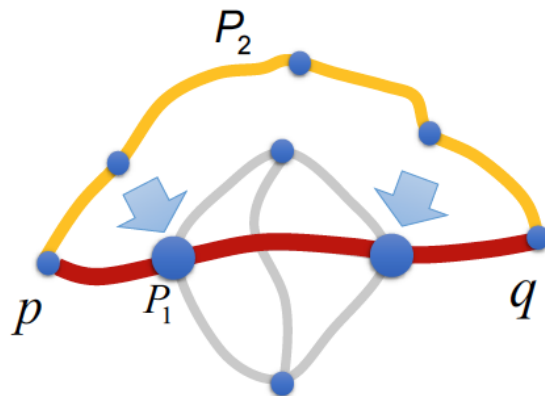


Figure 5: Explicit example Cartoon network where P_2 (highlighted in yellow) is a consolidated bypass of the shortest path P_1 (highlighted in red) since P_1 has smaller effective length than P_2 , despite of having a longer topological length. This happens because the shortest path involves some nodes with higher degree, which are sources where a walker could diffuse out.

S5 Validation on a toy network

S5.1 The toy network Let us put the formalism in action in a concrete example, a network of $n = 9$ nodes illustrated in Fig.5. In particular, P_1 is the shortest path connecting the nodes p and q (highlighted in red), and has topological length $\ell_{P_1} = 3$. This path however includes two ‘hubs’, prone to diffuse out particles (or to be damaged or jammed), and there exists an alternative route (P_2 , highlighted in yellow). P_2 is a potential bypass with larger topological distance $\ell_{P_2} = 4$.

S5.2 Topological length excess and ρ P_2 is indeed a consolidated bypass since $\mathbb{L}_{P_1} \approx 5.09$ and $\mathbb{L}_{P_2} \approx 4.80$, so $\mathbb{L}_{P_2} < \mathbb{L}_{P_1}$: while P_1 is topologically shorter, in units of the hidden resistive geometry, it is effectively longer! The topological length excess is $\epsilon_{(p,q)} = 100(1 - 3/4) = 25\%$, i.e. the walker will appear to be choosing a path with 25% more links than the shortest path.

Now, the effective distance per edge ratio

$$\rho = \frac{\mathbb{L}_{P_2}}{\ell_{P_2}} \cdot \frac{\ell_{P_1}}{\mathbb{L}_{P_1}} \approx 0.7073 < 0.75 = \frac{\ell_{P_1}}{\ell_{P_2}}.$$

In words, by actually choosing P_2 , the walker will only travel in each link a distance which is about 70% of the actual (effective) distance travelled via P_1 . This is less than 75%, the bound offered by the topological ratio. So the net saving of taking P_2 instead of the shortest path P_1 is indeed $100(1 - 0.7073) \approx 30\%$, but our lower bound offers a conservative $\epsilon = 25\%$.

Putting this example in a general context, this helps to illustrate the fact that by choosing the SRP over the SP, the walkers are reducing the effective length of their walk, therefore enhancing navigability. Our estimation of how much this is enhanced (ϵ) is only a conservative lower bound of the actual number.

S6 Hitting times and Excess times of SRP-like and SP-like random walkers

As explained in the paper, a free-flowing particle hopping randomly throughout the network is more likely to spread out and get lost through local connectivity paths (through the paths arising in intermediate nodes) if the path under study is proportionally more resistive.

Using random walks between a source node i and a destination node j can allow us to quantify the excess time needed to traverse different types of paths connecting i and j , and thus, in principle we can use random walk dynamics to illustrate the effect that bypasses have on network navigability by random walkers.

S6.1 Analysis in the toy network Since the toy network in Fig.5 is small, we can exhaustively analyse the statistics of random walkers. In particular, we have generated 10^5 random walkers starting at $i = p$ and monitor their node sequence until each of them ends at $j = q$, that is, we record the full sequence of nodes of a walker along its walk from p to eventually reaching q . Subsequently, each walker is then *classified* as a SRP-type or a SP-type depending on the

sequence of nodes they travel (this task is easy to do in the toy network, as for instance walkers travelling the SRP reach the destination from a node which is different from the one used if traversing the network via a SP region, see Fig.5). Once walkers have been classified, we then proceed to compare both classes by computing two magnitudes that proxy the time needed for the walker to reach destination and play the role of a dynamic (random-walk-like) analog of our network geometrization:

- The hitting time HT , defined as the total time required on average (average over all walkers in the same class) to reach the destination node q . This time is simply computed as the average size of the node sequences. It is a dynamic proxy for \mathbb{L} . To compare hitting times for both classes, we also compute the Hitting Time Ratio

$$HRT = \frac{HT_{\text{SRP-type}}}{HT_{\text{SP-type}}},$$

where $HRT < 1$ indicates that the net time spent by SRP-type walkers is lower than SP-type walkers.

- The Excess Time ET , that measures how much more time a random walker using e.g. the bypass needs due to the fact that it can backtrack or get lost in the vicinity of the bypass as compared to the time it would take if the walker was a ballistic one, i.e.

$$ET_{\text{SRP-type path}} = \frac{\langle HT_{\text{SRP-type}} \rangle}{\text{number of nodes in the SRP}}$$

$$ET_{\text{SP-type path}} = \frac{\langle HT_{\text{SP-type}} \rangle}{\text{number of nodes in the SP}}$$

Note that the excess time ET can be seen as a random-walk dynamics equivalent of the magnitude \mathbb{L}/ℓ , and thus in the same vein we have that $ET_{\text{SRP-type path}}/ET_{\text{SP-type path}}$ is the random-walk dynamics equivalent of the measure ρ (Eq.27).

- The Excess Time Saving ETS is a percentage that compares the Excess Time via SRP and SP:

$$ETS = \frac{ET_{\text{SP-type path}} - ET_{\text{SRP-type path}}}{ET_{\text{SRP-type path}}} \times 100$$

For the toy network, we find $\langle HT_{\text{SRP-type}} \rangle \approx 6.9$, whereas $\langle HT_{\text{SP-type}} \rangle \approx 10.9$, i.e. the hitting time is smaller for walkers of the SRP-type class than for the SP-type class. Similarly, we find $ET_{\text{SRP-type path}} \approx 1.38$, $ET_{\text{SP-type path}} \approx 2.7$, i.e. the time lost by SRP-type walkers due to their stochasticity is half of the time lost by SP-type walkers.

S6.2 Analysis in a real network We extend the previous analysis to a (larger) real network (functional –task-driven– brain network, see SI section on Empirical networks for details), composed by $n = 638$ nodes. We run 2×10^4 random walks between source i and destination j , for a total of $M = 20$ pairs of nodes (i, j) where we identified the SP and the SRP. Each of the walkers starts at i , makes a random excursion on the network, and eventually reaches j . Each walker is then *classified* as a SRP-type if all the nodes of the SRP are visited by the walker and none of the nodes of the SP is visited. Otherwise, the walker is classified as a SP-type if all the nodes in the SP are visited, but not all the SRP nodes are visited. The rest of the walkers are labelled as hybrid and not considered in the analysis. Finally, we compute the average hitting time and the excess time for each class and pair (i, j) , and the excess time saving for each pair (i, j) . Our results, depicted in Fig.6, indicate that the excess time of SP-like walkers is systematically larger than the excess time of SRP-like walkers, on agreement with previous results on the toy network. We find mixed results for the hitting times: for some pairs the average time spent is higher in the SP-type class, for some pairs it is higher in the SRP-type class. Finally, the excess time saving is systematically larger than 0, fluctuating between 25% and 225%. All in all, these results –while not exhaustive by any means– support and reinforce the idea that particles can get lost easier if random-walking through the SP than through the SRP.

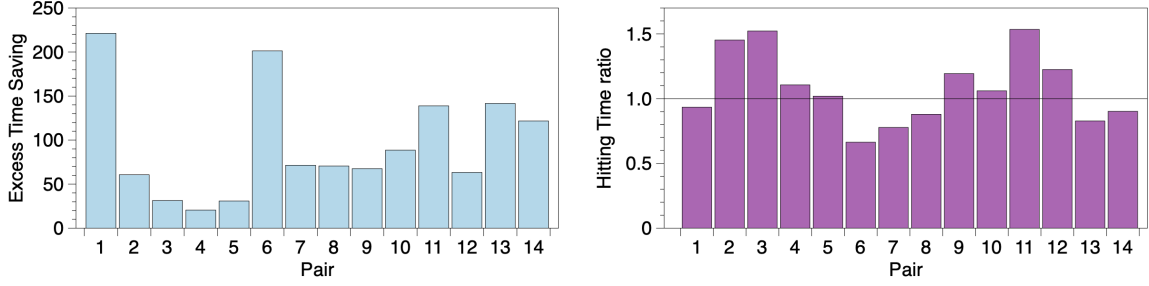


Figure 6: Excess Time Saving (left) and Hitting Time Ratio (right, see the text for details) for 14 out of 20 pairs of nodes in the brain network, for which there exist a SP and a SRP where SP-type and SRP-type walkers are found. Results are in agreement with the idea particles can get lost easier if random-walking through the SP than through the SRP.

S7 Further effects on dynamics: synchronization and epidemic spreading

S7.1 Synchronization The synchronizability of a network of coupled oscillators is governed by the Laplacian eigenratio μ_{\max}/μ_2 , where μ_{\max} and μ_2 are the largest and smallest (non-null) eigenvalues of the network’s Laplacian matrix, such that the smaller such eigenratio, the more synchronizable the network is. In panel (a) of Fig. 7 we illustrate the change of such eigenratio with the rewiring probability p in the Watts-Strogatz model. Interestingly, we find a qualitative change of behavior at $p^* \approx p_{\text{GNP}}$, where for $p < p^*$ the eigenratio scales as $\mu_{\max}/\mu_2 \sim p^{-\gamma}$, with $\gamma \approx 1.153$, whereas for $p > p^*$ the eigenratio’s behavior smoothly crossovers to a flat dependence. To derive the crossover value, we compute the sample standard deviation

$$s = \sqrt{\frac{\sum_{i=1}^{n(p^*)} (y_i - f(x_i))^2}{(n(p^*) - 1)}} \quad (29)$$

between the actual eigenratio and the scaling function above in the range $p < p^*$ and find the value p^* which minimises such error (see inset of panel (a) in Fig. 7). We find that the error in the fit is minimised for $p^* \approx 0.2$, indeed close to p_{GNP} .

S7.2 Epidemic spreading The second process is a SIR-type epidemic spreading over the network, where α is the birth rate of the epidemic and δ is its death rate. It is well known

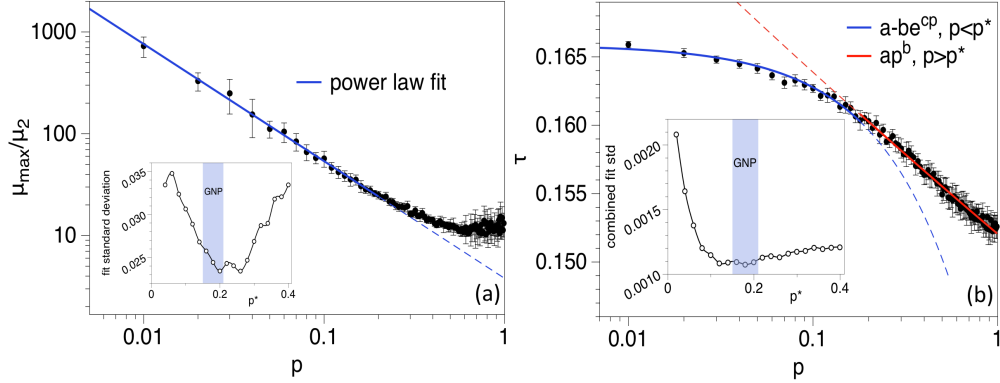


Figure 7: Dynamics. (a) Plot of the eigenratio μ_{\max}/μ_2 of the Laplacian matrix versus the rewiring probability p in a WS model with $N = 500$ nodes and average degree $k = 6$. The straight line corresponds to the power law decay of the eigenratio $\sim p^{-1.15}$. Note that the power law decay is a very good fit only in the range $0 < p < p^*$, thereafter smoothly crossovering to a flat dependence. (Inset) Sample standard deviation of the power law fit as a function of the upper bound p^* . This fitting error is minimized close to $p^* \approx p_{\text{GNP}}$, i.e. the crossover between a power law decay of the eigenratio and a flat dependence on p takes place at the network's Good Navigational Point, where bypasses have a maximal effect. (b) Plot of the epidemic threshold $\tau = 1/\lambda_1$ as a function of the rewiring probability p in the WS model with $N = 500$ nodes and average degree $k = 6$ (dots and error bars denote average and standard deviation over 100 realizations). The blue and red lines correspond to two qualitatively different fits, for $p < p^*$ (blue) and $p > p^*$ (red). (Inset) To find the value of p^* that marks the crossover between scaling behaviors, we compute the aggregate fit deviation of the two-function model, finding that such deviation reaches a minimum for $p^* \approx p_{\text{GNP}}$, i.e. the change of behavior onsets at the regime where bypasses take a predominant role.

that when $\alpha/\delta < \tau$ infection dies out and when $\alpha/\delta > \tau$ infection survives and becomes an epidemic, where τ is the epidemic threshold (the smallest τ , the easiest that an infection outbreak becomes epidemic). For undirected networks $\tau = 1/\lambda_1$, where λ_1 is the spectral radius of the adjacency matrix. As can be seen in panel (b) of Fig. 7 the epidemic threshold of a Watts-Strogatz network also shows a qualitative change: there is a crossover from a slow decrease for $p < p^*$ to a faster, power-law decrease for $p > p^*$. To find p^* , we compute the sample standard deviation of each branch (eq.29). The inset of panel (b) shows the combined sample standard deviations, that find a minimum for $p^* \approx p_{\text{GNP}}$. That is, up to the point in which bypasses become predominant, an infection is relatively easier to control than after that point.

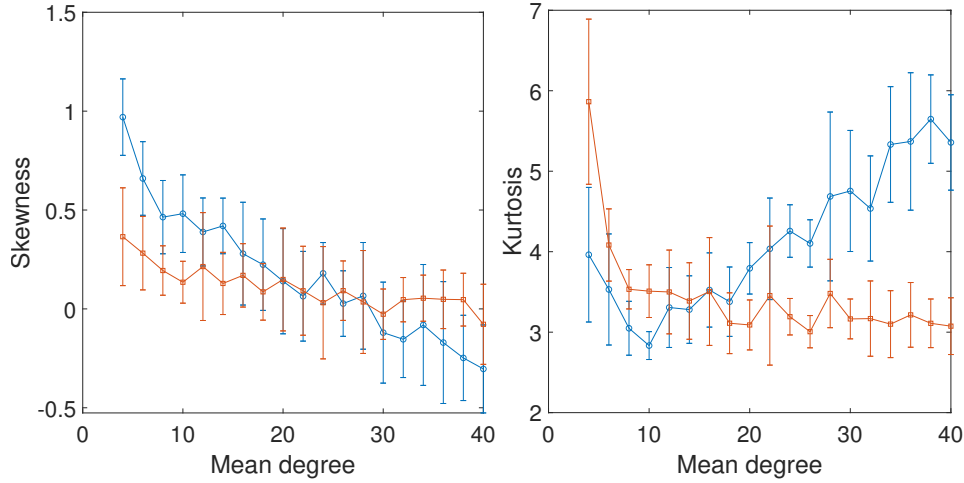


Figure 8: Plots of skewness (left) and kurtosis (right) of the degree distribution of ER networks and GNP-SW networks (with $p = p_{\text{GNP}} = 0.15$) as a function of their mean degree $\langle k \rangle$.

Altogether, these results suggest that dynamical processes running on the network perceive such bypasses in a nontrivial way, and these therefore play a role in the network’s function.

S8 Additional details on the ϵ vs $\langle k \rangle$ in ER and SW networks

Let us look at the degree distributions of the WS networks with $p = 0.15$ generated for very different $\langle k \rangle$. When $\langle k \rangle$ is relatively low the WS generates networks with a significant “tailedness” of the degree distribution. This is because a node with relatively low degree to which a small number of edges are removed from or added to, changes significantly its degree relative to the original one, e.g., a node of degree two to which two edges are added duplicates its degree relative to the original one. This effect is diluted, however, as soon as $\langle k \rangle$ increases. Therefore, for relatively small $\langle k \rangle$ we should find the existence of certain outlier nodes in terms of their degrees. This is exactly what it is observed when we consider the kurtosis of the degree distributions of WS networks (see Fig.8). For relatively small $\langle k \rangle$ the kurtosis of the degrees in SW networks is bigger than that of ER networks. When $\langle k \rangle > 16$ this relation is inverted and ER displays more “tailedness” than the WS degrees.

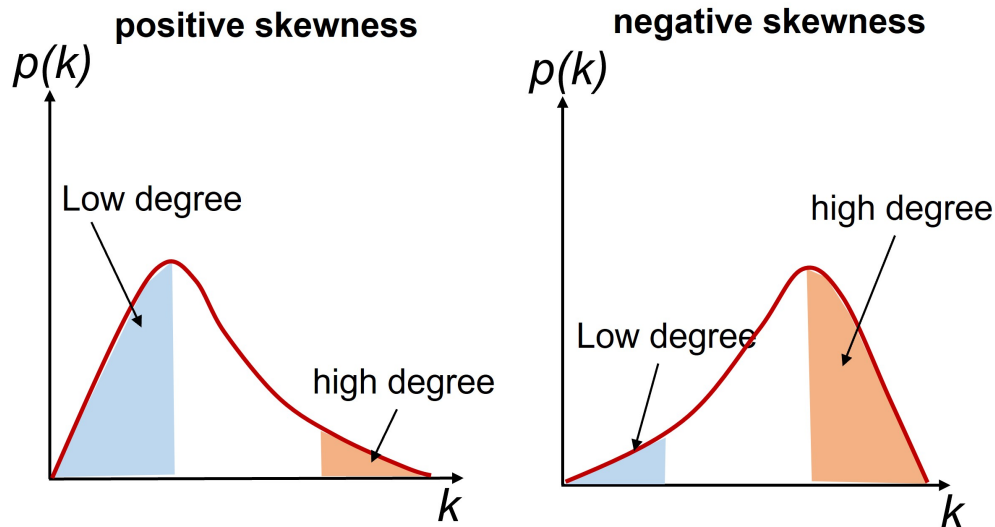


Figure 9: A sketch of the degree distribution with positive and negative skewness respectively, and the relative abundance of low and high degree nodes.

But this is not the end of the story. The asymmetry of the degree distribution of an ER network also changes dramatically when $\langle k \rangle$ increases. For $\langle k \rangle \leq 30$ the skewness of the degree in ER networks is positive, and indeed bigger than that of a WS network of comparable size. This means the existence of significantly more low degree nodes than hubs, i.e., it looks like a mini-power-law. However, for $\langle k \rangle > 30$ the skewness of the degrees in ER become negative and smaller than that of WS, which remains positive (see Fig.9 for a sketch). This gives again advantages to WS networks to avoid these few hubs existing in it and using bypasses. However, the ER now have much more high degree nodes than low degree ones, making impossible to have bypasses. Does a GNP exists for this regime, $\langle k \rangle > 30$, and if so is it at $p = 0.15$? The answer to both questions is positive.

S9 Super-hubs and the transition to ultra-short graphs

As we have seen the preferential attachment method produces significantly more bypasses than a random interconnection of nodes. The question that emerges is if there is a simple mechanism

which produces even more bypasses than those introduced by the skew degree distribution of the BA method. Let us consider a sparse connected random graph G (see Fig. 10). The chances that there are some bypasses in G are scarce, so we can consider that such number is null. As the graph G is connected there is a SP between every pair of nodes. Now, let us create G' by adding a new node connected to every node of G . This new node v is a super-hub, which is connected to $n' - 1$ nodes, where n' is the number of nodes in G' . Therefore, a particle trying to go from one node $i \neq v$ to another $j \neq v$ will avoid going through the super-hub as this will be a very resistive trajectory. However, the particle can travel by using the SP connecting them in G . For instance, it can go through the path: $1 - 2 - 5$, $1 - 2 - 5 - 6$, $1 - 2 - 5 - 4$, $1 - 2 - 5 - 4 - 3$ instead of through the paths $1 - 2 - j$. Consequently, all those paths which are of length larger than 2 become potential bypasses by the effect of the newly added super-hub. Due to the shape of the graph illustrated in Fig. 10 we call this the “umbrella effect”, and relates to the transition to ultra-short graphs. In closing, this mechanism potentially transforms all SP of length larger than 2 in a sparse graph into bypasses.

This effect is expected to occurs in the BA mechanism when the mean degree k_{mean} of the network is large. That is, suppose that at certain “time” t of the BA evolutionary mechanism, the number of existing nodes n_t is smaller than $\langle k \rangle$. This frequently happens at the initial stages of the evolution of BA networks when $\langle k \rangle$ is relatively large. In these cases, the new nodes attached to the network need to be connected to every existing node in the graph, producing an umbrella effect during these periods of the process. The resulting effect could be an explosion of bypasses in the final BA network when $\langle k \rangle$ is relatively large.

S10 Discussion on weighted networks

When we consider a generalized communicability distance $\xi_{ij}(\beta) = \sqrt{G_{ii}(\beta) + G_{jj}(\beta) - 2G_{ij}(\beta)}$, the values of the three terms involved in $\xi_{ij}(\beta)$ change nonlinearly with β . Consequently, there

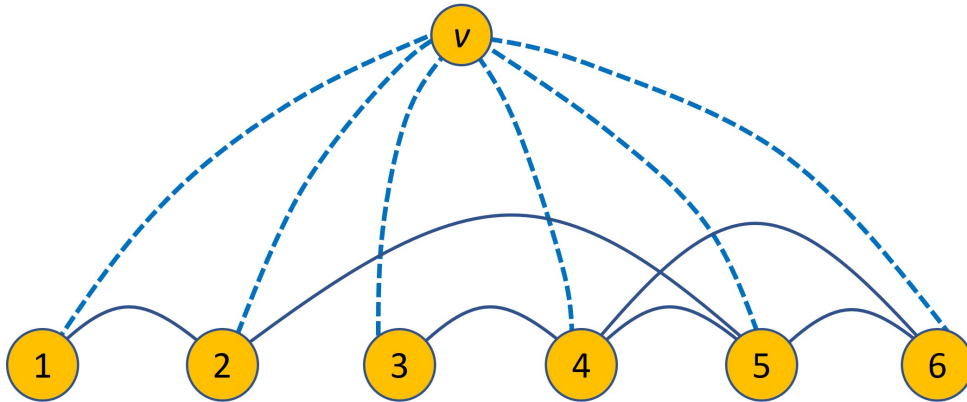


Figure 10: Illustration of the umbrella effect. Initially we have a simple sparse connected network G with 6 nodes and 6 edges. A new graph G' is created by adding a node connected to every existing node of G . This new super-hub makes all previous paths in the original network to be bypasses of the shortest paths, that now involve the super-hub. Adding this super-hub makes ϵ to experience a sudden increase, what we call the umbrella effect.

will be effects on the lengths of the paths studied which depends on this parameter. To illustrate this situation let us consider our toy network in which we have found that $\epsilon = 0.6944$ due to the existence of the bypass 1-9-8-7-4. If we multiply the adjacency matrix by 0.5, i.e., we change the weight of every edge from 1.0 to 0.5. In this case we obtain $\epsilon = 0$, which means that the bypass no longer exists. This means that if we reduce the weight of every edge by a half, it is no longer “economic” for a walker to use the path 1-9-8-7-4 instead of the path 1-2-3-4. The fact is that when $\beta = 1$ the communicability distance between 2 and 3 is slightly longer than that between 8 and 9. However, when $\beta = 0.5$ both distances are identical, such that it is shorter (in terms of communicability distances) going through the topological SP. We use this example to find the meaning of the edge weights in the context of communicability distances. For that we can use the metaphor that the edge weight represents the “width” of the edge like if it were a street connecting two intersections. The influence of this width is twofold. For instance, suppose that two nodes i and j are connected by an edge with weight equal to 2. This means that we have doubled the width of the street by adopting two lanes to connect the pair

of nodes. It is evident that this will increase the communicability G_{ij} between the two nodes as well as of those in any path containing that edge. However, the “complexity” of the intersections i and j is also increased, which means an increase in the values of G_{ii} and G_{jj} . The distance ξ_{ij} will depend on how much each of these terms, G_{ij} or G_{ii} and G_{jj} , increases more. A similar situation emerges if we consider that the edge weight is for instance 0.1, which indicates that we have dropped the width of the corresponding street. This drop in the edge weight produces a decrease in the three terms implied in the definition of the communicability distance. Consequently, it will depend on the topological characteristics of the nodes and edge involved whether the distance decrease significantly or not in relation to the unweighted case.

In order to be able to compare a weighted and an unweighted network we need to normalize the weights of a network such as their mean is unity coinciding with the mean weight of the edges in a non weighted network. This is what we do in the next examples considering weighted networks. Let us now provide some numerical examples based on our toy model. First, let us consider the edge 8 – 9 which is in the SCP but not in the SP. If we increase the value of this weight, for instance to values between 1.5 to 2.0, we obtain that $\epsilon = 0$, indicating that there is no longer a bypass between the nodes 1 and 4. In this case any particle traveling between the nodes 1 and 4 will prefer to go through the SP. This result indicates that here the increase in the self-communicabilities of the nodes 8 and 9 is more significant than the increase of the communicability between the two nodes. As a consequence the communicability distance between the nodes 8 and 9 increases significantly making the traveling through them more difficult than through the SP. If we drop the value of this weight between 0.1 and 1.4, the increase of the communicability distance between 8 and 9 is not enough as to make the traveling more efficient through the SP. Consequently, we obtain $\epsilon = 0.6944$, indicating the existence of a bypass.

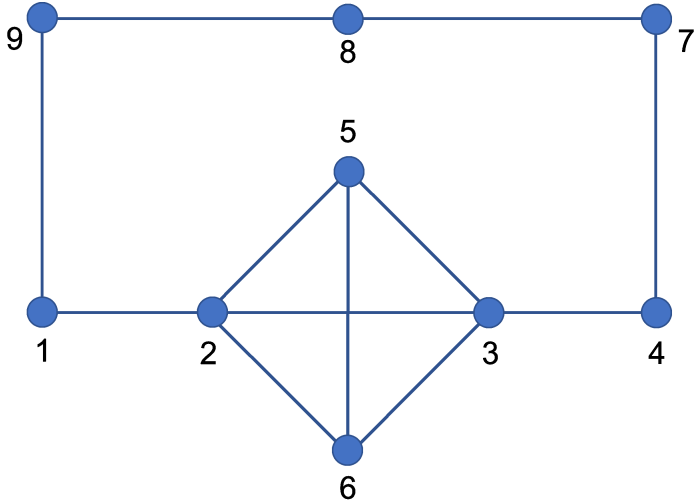


Figure 11: Toy network with node labelling.

To illustrate the complexities of this problem let us increase the weight of this edge too much as to facilitate even more the navigation through the SP connecting the nodes 1 and 4. For instance, if we increase this weight up to 10, it is true that a walker travelling between 1 and 4 will go through the SP connecting them. However, the result of the whole network is that $\epsilon = 0.6944$. This indicates that another bypass has emerged. This occurs for a particle traveling between 1 and 7, for which it is preferable to go through the path 1-2-3-4-7 than through the path 1-9-8-7, because of the large weight of an edge in the second path.

To continue illustrating the nontriviality of the influence of edge weights on the communicability distance let us select the weight between the nodes 2 and 3. This edge is in the SP between nodes 1 and 4 and not in the SCP. Dropping this weight will facilitate the navigation through the SP. The question is whether this effect is enough as for the particle to prefer to go through the path 1-2-3-4 than through the bypass 1-9-8-7-4. The answer is not. If we drop this weight to 0.1 we find $\epsilon = 0.6944$ and the bypass between the two nodes remains. Not even dropping it to 10^{-12} makes any difference. The question is that the node 2 is still connected to three other nodes with a weight equal to one, which still keep a large weighted self-communicability for

this node due to its implication in triangles, squares, etc. To make that the bypass disappears we need to change the weights of the 6 edges in the central clique of the graph. In this case, if for instance, we drop their weights to 0.1, the bypass no longer exists and the particle will travel through the SP. What happened here is that by changing the weights of all edges in the clique we have reduced significantly the values of the self-communicabilities of the nodes 2 and 3 as to make that the communicability distance drops significantly enough as to facilitate the navigation through this path.

S11 Empirical networks

S11.1 Additional details on empirical networks Below we provide details on all empirical networks, grouped by topic (see also table 2 for a summary of some characteristics).

Brain networks

- **Neurons:** Neuronal synaptic network of the nematode *C. elegans*. Included all data except muscle cells and using all synaptic connections [70]
- **Human brain (anatomical) [71]:** Structural connectivity network of 70 healthy volunteers studied by Hagmann et al. The nodes of these networks correspond to 1,000 physical regions in the brain and the connections among them were estimated for individual participants using deterministic streamline tractography, such that they represent physical connections between brain areas.
- **Human brain (functional, resting-state) [71]:** We then studied the functional brain networks for the same 70 individuals studied while participants were not engaged in any overt task, such that the scans are treated as eyes-open resting-state fMRI among the same 1,000 brain regions studied before. In this case we used a threshold for each brain

network such that the resulting webs had the same edge densities than the corresponding structural connectivity ones.

- **Human brain (functional, task-driven):** task-related coactivation brain network Although this network has a different parcellation than the previous two ones (consisting on 638 brain regions), this is the product of a meta-analysis of the large primary literature that used fMRI or PET to measure task-related activation (meta-analysis of over 1,600 studies published between 1985–2010 [72]).

Ecological networks

- **Benguela:** Marine ecosystem of Benguela off the southwest coast of South Africa [73]
- **Bridge Brook:** Pelagic species from the largest of a set of 50 New York Adirondack lake food webs [74];
- **Canton Creek:** Primarily invertebrates and algae in a tributary, surrounded by pasture, of the Taieri River in the South Island of New Zealand [75];
- **Chesapeake Bay:** The pelagic portion of an eastern U.S. estuary, with an emphasis on larger fishes [76];
- **Coachella:** Wide range of highly aggregated taxa from the Coachella Valley desert in southern California [77];
- **El Verde:** Insects, spiders, birds, reptiles and amphibians in a rainforest in Puerto Rico [78];
- **Grassland:** all vascular plants and all insects and trophic interactions found inside stems of plants collected from 24 sites distributed within England and Wales [79];

- **Little Rock:** Pelagic and benthic species, particularly fishes, zooplankton, macroinvertebrates, and algae of the Little Rock Lake, Wisconsin, U.S. [80];
- **Reef Small:** Caribbean coral reef ecosystem from the Puerto Rico-Virgin Island shelf complex [81];
- **Scotch Broom:** Trophic interactions between the herbivores, parasitoids, predators and pathogens associated with broom, *Cytisus scoparius*, collected in Silwood Park, Berkshire, England, UK [82];
- **Shelf:** Marine ecosystem on the northeast US shelf [83];
- **Skipwith:** Invertebrates in an English pond [84];
- **St. Marks:** Mostly macroinvertebrates, fishes, and birds associated with an estuarine seagrass community, *Halodule wrightii*, at St. Marks Refuge in Florida [85];
- **St. Martin:** Birds and predators and arthropod prey of *Anolis* lizards on the island of St. Martin, which is located in the northern Lesser Antilles [86];
- **Stony Stream:** Primarily invertebrates and algae in a tributary, surrounded by pasture, of the Taieri River in the South Island of New Zealand in native tussock habitat [87];
- **Ythan1:** Mostly birds, fishes, invertebrates, and metazoan parasites in a Scottish Estuary [88];
- **Ythan2:** Reduced version of Ythan1 with no parasites [89].
- **Termite:** The networks of three-dimensional galleries in termite nests [90];

Informational networks

- **Roget:** Vocabulary network of words related by their definitions in Roget's Thesaurus of English. Two words are connected if one is used in the definition of the other [91];

Biological networks

- **Protein-protein interaction networks** in: *S. cerevisiae* (yeast) [92, 93];
- **TransE.coli, Transyeast:** Direct transcriptional regulation between genes in *Saccharomyces cerevisiae*. [70, 94].

Social networks

- **Geom:** Collaboration network of scientists in the field of Computational Geometry [96];
- **QcGr** Collaboration network of scientists in the field of Quantum Gravity [97];
- **Drugs:** Social network of injecting drug users (IDUs) that have shared a needle in the last six months [98];

Technological and infrastructural networks

- **Electronic:** Three electronic sequential logic circuits parsed from the ISCAS89 benchmark set, where nodes represent logic gates and flip-flop [70];
- **USAir97:** Airport transportation network between airports in US in 1997 [96];
- **Internet:** The internet at the Autonomous System (AS) level as of September 1997 [99];
- **Power Grid:** The power grid network of the Western USA [100].

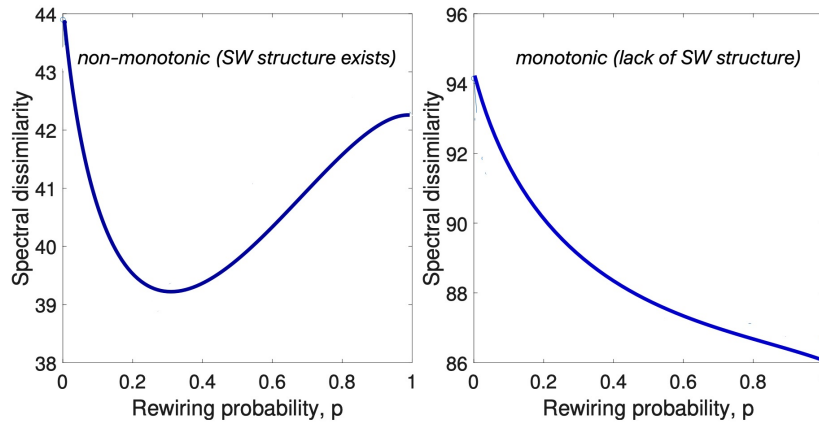


Figure 12: Typical dissimilarity plots obtained in the analysis of empirical networks: we either we find a non-monotonic behavior that highlights an optimal value at intermediate values of p (left panel) or a monotonically decreasing function, for which $p^* = 1$ (right panel). The former suggests a clear SW structure while the latter suggests that the network is closer to a random graph.

Software networks

- Collaboration networks associated with six different **open-source software** systems, which include collaboration graphs for three Object Oriented systems written in C++, and call graphs for three procedural systems written in C. The class collaboration graphs are from version 4.0 of the **VTK** visualization library; the CVS snapshot dated 4/3/2002 of Digital Material (DM), a library for atomistic simulation of materials; and version 1.0.2 of the AbiWord word processing program. The call graphs are from version 3.23.32 of the **MySQL** relational database system, and version 1.2.7 of the **XMMS** multimedia system. Details of the construction and/or origin of these networks are provided in Myers [101].

S11.2 Additional details on calculation of p^* As can be seen in table 1 of the main article, we find two classes of networks, one class is formed by networks for which a minimum dissimilarity exists between the real-world network and a WS model operating close to p_{GNP} (see Fig. 12, left panel). The other class is formed by networks which are more similar to the random

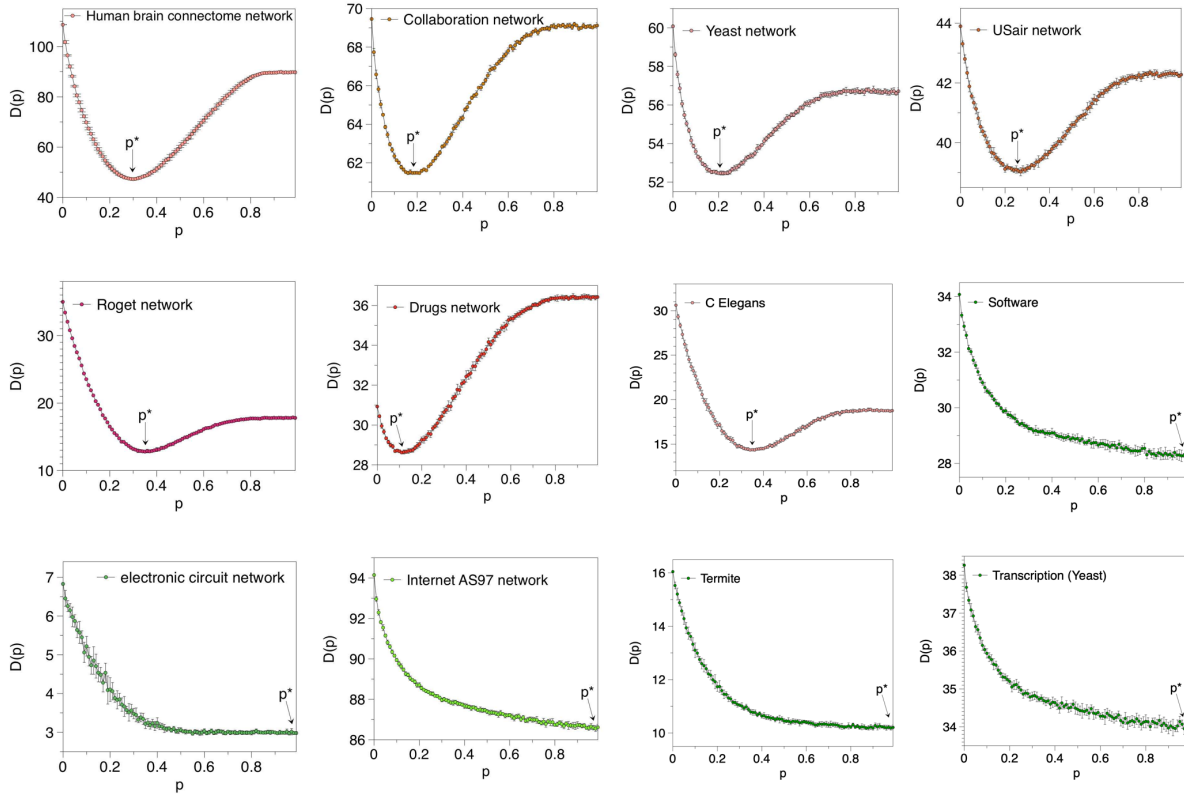


Figure 13: Dissimilarity curves $\mathcal{D}(p)$ as a function of the rewiring probability p , for different empirical networks: biological (human brain, C-elegans, protein-protein interaction, transcription, termite mound), social (drugs, scientific collaboration, Roget thesaurus), technological (airports, Internet AS, software, electronic circuits). The minimum of these curves characterizes the type of SW network which is more similar to the empirical network.

graph, i.e., WS with $p = 1$ (see Fig. 12 right panel). The dissimilarity curve is plotted for some empirical networks in Fig. 13.

S11.3 ϵ and ϵ/ϵ_{BA} : further analysis Here we give a closer inspection into the values of table 1 of the main article. Overall, we can see that for a groups of networks (not necessarily domain specific), the bypass navigability gain ϵ is similar to the one expected for a BA model with the same number of nodes N and mean degree $\langle k \rangle$, suggesting that the type of heterogeneity is similar and that the contribution of bypasses is substantial due to the presence of hubs. This is the case, for instance, in the Human brain, collaboration networks, C. Elegans neurons, or USA

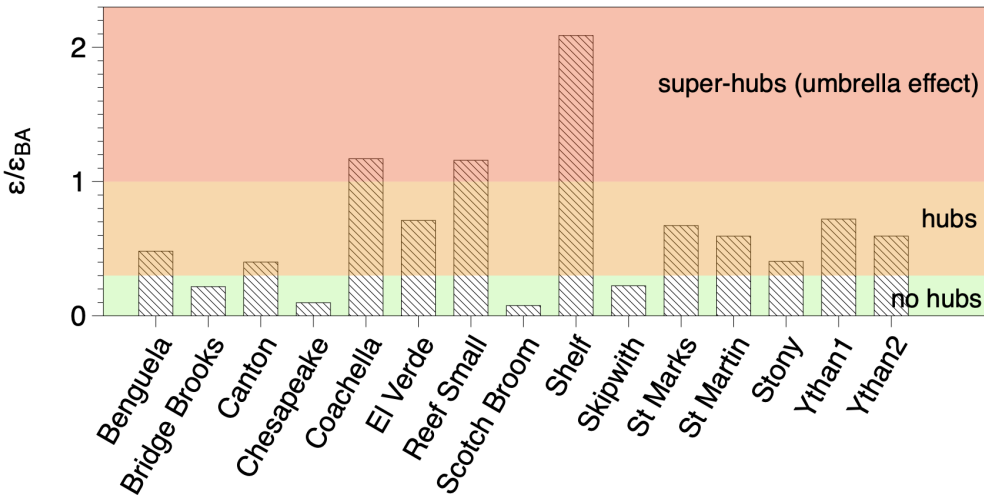


Figure 14: ϵ/ϵ_{BA} for all 15 food webs. We have highlighted three regimes: $\epsilon/\epsilon_{BA} < 0.5$, where the network is essentially not bypassing hubs, $0.5 < \epsilon/\epsilon_{BA} < 1$, where the real network and its analogous BA network have fairly similar associated navigability gain and thus the real network is bypassing hubs, and $\epsilon/\epsilon_{BA} > 1$ where the real network is bypassing hubs stronger than in the BA model. This last situation takes place when super-hubs emerge, i.e. nodes that connect to a large portion of the rest of nodes in the network.

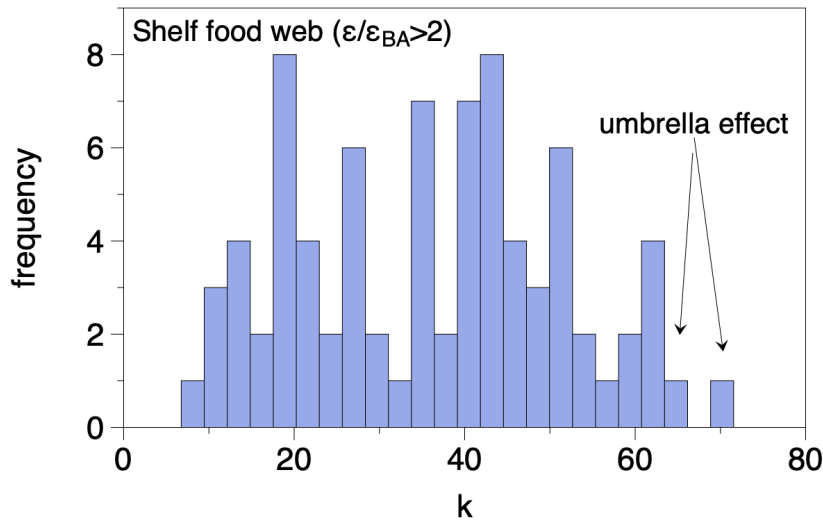


Figure 15: Degree frequency histogram of the Shelf food web (the one with $\epsilon/\epsilon_{BA} > 2$). This network has $N = 81$ nodes and a large number of them have very high degree. Some of these nodes will convert into super-hubs and then be likely to evidence the umbrella effect (see SI section S6) which make the navigability gain ϵ larger than the expected for a BA network.

airports: for all these cases $\epsilon/\epsilon_{BA} > 0.75$.

There is a second group of networks where such ratio is lower, suggesting that either the role of hubs is, at least, less prominent than what we would expect in a BA model with the same characteristics, or that even if hubs exist, the network is designed to not bypasses. In this group we find a whole spectrum of values ϵ : networks where the role of bypasses is still substantial but considerably less than in a comparable BA model (e.g. protein-protein interaction, with $\epsilon \approx 25$, with $\epsilon/\epsilon_{BA} \approx 0.55$), and networks where the bypasses have only a marginal effect in the network's navigability (e.g. termite mounds, with $\epsilon \approx 3$, with $\epsilon/\epsilon_{BA} \approx 0.12$, or the power grid, with $\epsilon \approx 2.6$, with $\epsilon/\epsilon_{BA} \approx 0.05$). The result on the power grid is interesting: originally seen as an example of a scale-free network [4] (albeit with an exponent 4, i.e. much more homogeneous than a BA network), its scale-freeness has been a matter of debate [62]. Nevertheless, it is clear that this network do have hubs. So our measures –that highlights that this network has bypasses have only about 5% of the impact than a respective BA network would have– determine that this network is not engineered to have routes bypassing hubs. This is in agreement to previous evidence on blackouts and cascading failures in such type of networks: these are examples of networks with fat-tailed degree distributions that do not follow an evolutionary process, which would certify the presence of bypasses.

Next, we disaggregate the calculation of ϵ/ϵ_{BA} performed on the 15 food webs. In Fig. 14 we plot the estimate of ϵ/ϵ_{BA} in each of them, where ϵ_{BA} is computed by generating BA models with the same number of nodes and mean degree that the empirical network, and averaging the resulting value of the navigability gain over 100 realizations of the BA model. We find food-webs across three regimes: the regime of low ϵ/ϵ_{BA} , which indicates that the network does not have hubs or that the network has not been designed to bypass these, the regime where $\epsilon \approx \epsilon_{BA}$, which indicates that the network is compatible with a BA model and the navigability gain is

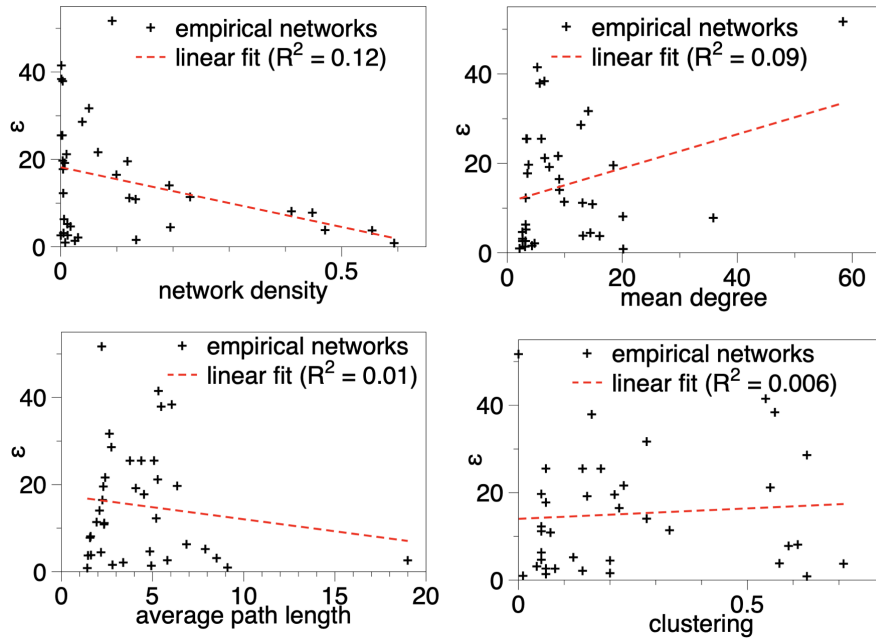


Figure 16: Scatter plots of ϵ vs standard network metrics, along with linear regression estimates. In all cases the R^2 coefficient is rather low, certifying that ϵ is not trivially reduceable to more basic network measures.

therefore associated to hubs being bypassed, and a (new) third regime ϵ/ϵ_{BA} , found for very dense networks, where there are some nodes in the empirical network that likely evidence the umbrella effect. Figure 15 illustrates this fact for the case of the Shelf food web ($\epsilon/\epsilon_{BA} > 2$). In this figure we plot the degree frequency of this food web, showing that this is a notably dense network where we find some nodes with extreme degree (note that this network has $N = 81$ nodes) which are candidates for the umbrella effect.

S11.4 Lack of correlation between ϵ and standard network metrics In Fig.16 we plot scatter plots of ϵ vs standard network metrics (network density, mean degree, average path length and average clustering) for all empirical networks analysed, showing that no trivial correlation emerges, specially in the region of lower density. In this sense, our results are not trivially reduceable to other standard network metrics.

References

- [1] Estrada, E (2012) *The structure of complex networks: theory and applications* (Oxford University Press, Oxford, UK).
- [2] Latora, V, Nicosia, V, Russo, G (2017) *Complex networks: principles, methods and applications* (Cambridge University Press, Cambridge, UK).
- [3] Watts, DJ., Strogatz, SH (1998) Collective dynamics of ‘small-world’ networks. *Nature* 393, 6684 (1998): 440-442.
- [4] Barabasi, A.L., and Albert, R. Emergence of scaling in random networks. *Science* 286, 5439 (1999): 509-512.
- [5] Tranquillo, J (2019) *An Introduction to Complex Systems. Making Sense of a Changing World* (Springer-Nature, Switzerland) pp. 314-315.
- [6] Arthur, WB (1994) *Increasing Returns and Path Dependence in Economy* (University of Michigan Press, Ann Arbor, USA).
- [7] Broido, AD, Clauset, A (2019) Scale-free networks are rare. *Nature Communications* 10, 1-10.
- [8] Holme, P (2019) Rare and everywhere: Perspectives on scale-free networks. *Nature communications*, 10, 1-3.
- [9] Xiao, X, Chen, H, Bogdan, P (2021) Deciphering the generating rules and functionalities of complex networks. *Sci. Rep.* 11, 22964.
- [10] Albert, R., Jeong, H., and Barabasi, A. L. (2000). Error and attack tolerance of complex networks. *Nature* 406, 6794: 378-382.

- [11] Xue, Y, Bogdan, P (2017) Reliable Multi-Fractal Characterization of Weighted Complex Networks: Algorithms and Implications. *Sci. Rep.* 7, 7487.
- [12] Gómez-Gardeñes, J, Latora, V (2008) Entropy rate of diffusion processes in complex networks. *Physical Review E* 78, 065102.
- [13] Sneppen, K, Trusina, A, and Rosvall, M (2005) Hide-and-seek on complex networks. *EPL (Europhysics Letters)* 69, 853.
- [14] Rosvall, M, Gronlund, A, Minnhagen, P, Sneppen, K (2005) Searchability of networks. *Physical Review E* 72, 046117.
- [15] Sporns, O (2011) *Networks of the brain* (MIT Press, Cambridge, USA).
- [16] Goñi, J, van den Heuvel, MP, Avena-Koenigsberger, A, Velez de Mendizabal, N, Betzel, RF, Griffa, A, Hagmann, P, Corominas-Murtra, B, Thiran, J-P, Sporns, O (2013) Resting-brain functional connectivity predicted by analytic measures of network communication. *Proceedings of the National Academy of Sciences* 111, 833-838.
- [17] Estrada, E (2021) Informational cost and networks navigability. *Applied Mathematics and Computation* 397, 125914.
- [18] Von Luxburg, U, Radl, A, Hein, M (2010) Getting lost in space: Large sample analysis of the commute distance. *Advances in neural information processing systems* 23, 2622-2630.
- [19] Berthier, E, Porter, MA, Daniels, KE (2019) Forecasting failure locations in 2-dimensional disordered lattices. *Proceedings of the National Academy of Sciences* 116, 6742-16749.
- [20] Echenique, P, Gómez-Gardeñes, J, Moreno, Y (2005) Dynamics of jamming transitions in complex networks. *EPL (Europhysics Letters)* 71, 325.

- [21] Lacasa, L, Cea, M, Zanin, M (2009) Jamming transition in air transportation networks. *Physica A* 388, 3948-3954.
- [22] Duch, J, Arenas, A (2006) Scaling of fluctuations in traffic on complex networks. *Physical Review Letters* 96, 218702.
- [23] Zhao, L, Lai, YC, Park, K, Ye, N (2005) Onset of traffic congestion in complex networks. *Physical Review E* 71, 026125.
- [24] Gosak, M, Milojević, M, Duh, M, Skok, K, Perc, M (2022) Networks behind the morphology and structural design of living systems. *Physics of Life Reviews* 41, 1-21.
- [25] Bassett, DS, Bullmore, ED (2006) Small-world brain networks. *The neuroscientist* 12, 512-523.
- [26] Van den Heuvel, MP, Sporns, O (2013) Network hubs in the human brain. *Trends in Cognitive Sciences* 17, 683-696.
- [27] Dardo, T, Wang, G-J, Volkow, ND (2013) Energetic cost of brain functional connectivity. *Proceedings of the National Academy of Sciences* 110, 13642-13647.
- [28] Caio, S, Van Den Heuvel, MP, Zalesky, A (2018) Navigation of brain networks. *Proceedings of the National Academy of Sciences* 115, 6297-6302.
- [29] Avena-Koenigsberger, A, Misic, B, Sporns, O (2018) Communication dynamics in complex brain networks. *Nature Reviews Neuroscience* 19, 17-33.
- [30] Yin, C, Xiao, X, Balaban, V, Kandel, ME, Lee, YJ, Popescu, G, Bogdan, P (2020) Network science characteristics of brain-derived neuronal cultures deciphered from quantitative phase imaging data. *Scientific reports* 10, 15078.

- [31] Klein, D, Randic, M (1993) Resistance distance. *Journal of Mathematical Chemistry* 12, 81-95.
- [32] Grippo, E, Jonckheere, EA (2016) Effective resistance criterion for negative curvature: application to congestion control. *IEEE Conference on Control Applications* 129-136.
- [33] Jonckheere, E, Grippo, E, Banirazi, R (2019) Curvature, entropy, congestion management and the power grid. *IEEE Conference on Control Technology and Applications* 535-542.
- [34] Von Luxburg, U, Radl, A, Hein, M (2010) Getting lost in space: Large sample analysis of the commute distance. *Advances in neural information processing systems* 23, 2622-2630.
- [35] Faber, JE, Chilian, WM, Deindl, E, van Royen, N, Simons, MA (2014) Brief etymology of the collateral circulation. *Arteriosclerosis, thrombosis, and vascular biology* 34, 1854-1859.
- [36] Ahuja, Ravindra K., Thomas L. Magnanti, and James B. Orlin. *Network flows*. (1988, MIT).
- [37] Estrada, E, Hatano, N (2008) Communicability in complex networks. *Physical Review E* 77, 036111.
- [38] Estrada, E, Hatano, N, Benzi, M (2012) The physics of communicability in complex networks. *Physics Reports* 514, 89-119.
- [39] Estrada, E., & Hatano, N. Statistical-mechanical approach to subgraph centrality in complex networks. *Chemical Physics Letters* 439 (2007), 247-251.
- [40] Lee, C. H., Tenneti, S., & Eun, D. Y. Transient dynamics of epidemic spreading and its mitigation on large networks. In *Proceedings of the twentieth ACM international symposium on mobile ad hoc networking and computing* 2019 (pp. 191-200).

- [41] Bartesaghi, P., & Estrada, E. Where to cut to delay a pandemic with minimum disruption? Mathematical analysis based on the SIS model. *Mathematical Models and Methods in Applied Sciences* 31, 12 (2021), 2571-2596.
- [42] Arola Fernandez, L. Synchronization in Complex Networks Under Uncertainty (Doctoral dissertation, Universitat Rovira i Virgili, 2022). Chapter 6.
- [43] Zamani Esfahlani, F., Faskowitz, J., Slack, J., Masic, B., and Betzel, R. F. Local structure-function relationships in human brain networks across the lifespan. *Nature Communications*, 13, 1 (2022), 1-16.
- [44] Arnatkeviciute, A., Fulcher, B. D., Oldham, S., et al. Genetic influences on hub connectivity of the human connectome. *Nature Communications* 12, 1 (2021), 1-14.
- [45] Crofts, Jonathan J., and Desmond J. Higham. A weighted communicability measure applied to complex brain networks. *Journal of the Royal Society Interface* 6, 33 (2009): 411-414.
- [46] Crofts, J. J., Higham, D. J., Bosnell, R., Jbabdi, S., Matthews, P. M., Behrens, T. E. J., and Johansen-Berg, H. Network analysis detects changes in the contralesional hemisphere following stroke. *Neuroimage* 54, 1 (2011): 161-169.
- [47] Campbell, I. M., James, R. A., Chen, E. S., and Shaw, C. A. NetComm: a network analysis tool based on communicability. *Bioinformatics* 30, 23 (2014).
- [48] Lella, E., Amoroso, N., Lombardi, A., Maggipinto, T., Tangaro, S., Bellotti, R., and Alzheimer's Disease Neuroimaging Initiative. Communicability disruption in Alzheimer's disease connectivity networks. *Journal of Complex Networks* 7, 1 (2019): 83-100.

- [49] Betzel, R. F., Gu, S., Medaglia, J. D., Pasqualetti, F., and Bassett, D. S. Optimally controlling the human connectome: the role of network topology. *Scientific Reports* 6, 1 (2016): 1-14.
- [50] Seguin, C., Sporns, O., Zalesky, A., and Calamante, F. Network communication models narrow the gap between the modular organization of structural and functional brain networks. *NeuroImage*, 119323 (2022).
- [51] Serra-Musach, Jordi, et al. Cancer network activity associated with therapeutic response and synergism. *Genome Medicine* 8, 1 (2016): 1-12.
- [52] Mander, L., Dekker, S. C., Li, M., Mio, W., Punyasena, S. W., and Lenton, T. M. A morphometric analysis of vegetation patterns in dryland ecosystems. *Royal Society Open Science* 4, 2 (2017): 160443.
- [53] Li, Y., Zobel, C. W., Seref, O., and Chatfield, D. Network characteristics and supply chain resilience under conditions of risk propagation. *International Journal of Production Economics* 223, 107529 (2020).
- [54] Estrada, E., Every nonsingular spherical Euclidean distance matrix is a resistance distance matrix. *Linear Algebra and its Applications* 656 (2023): 198-209.
- [55] S. Markvorsen, S., Minimal webs in Riemannian manifolds. *Geometriae Dedicata* 133, 1 (2008): 7-34.
- [56] Bridson, M. R., & Haefliger, A. Metric spaces of non-positive curvature (Vol. 319) (2013, Springer Science & Business Media).
- [57] Yang, H., Zhao, F., Wang, B., Synchronizabilities of networks: a new index, *Chaos* 16, 043112 (2006).

- [58] Zhu, G., Yang, H., Yin, C. Li, B., Localizations on complex networks, *Physical Review E* 77, 066113 (2008).
- [59] Del Genio, C. I., Gross, T., & Bassler, K. E. All scale-free networks are sparse. *Physical Review Letters* 107, 17 (2011).
- [60] G. Zamora-López and R. Brasselet, Sizing complex networks. *Comms. Physics* 2:144 (2019).
- [61] Walker, D. M., and Tordesillas, A. Topological evolution in dense granular materials: a complex networks perspective. *International Journal of Solids and Structures* 47, 5 (2010). 624-639.
- [62] Hartmann, B., & Sugar, V., Searching for small-world and scale-free behaviour in long-term historical data of a real-world power grid. *Scientific Reports* 11, 1 (2021): 1-10.
- [63] Mei, S., Zhang, X., & Cao, M. *Power grid complexity* (Springer Science & Business Media, 2011).
- [64] G. Rapisardi, I. Kryven, and A. Arenas, Percolation in networks with local homeostatic plasticity, *Nature Communications* 13, 1 (2022): 1-9.
- [65] F. Battiston, F. G. Cencetti, I. Iacopini, V. Latora, M. Lucas, A. Patania, J.G. Young, and G. Petri. Networks beyond pairwise interactions: structure and dynamics. *Physics Reports* 874 (2020): 1-92.
- [66] Majhi, S., Perc, M., and Ghosh, D. (2022). Dynamics on higher-order networks: A review. *Journal of the Royal Society Interface* 19 (188), 20220043.
- [67] Akbarzadeh, M, Estrada, E (2018) Communicability geometry captures traffic flows in cities. *Nature Human Behaviour* 2,645-652.

- [68] Goñi, J., Avena-Koenigsberger, A., Velez de Mendizabal, N., van den Heuvel, M. P., Betzel, R. F., & Sporns, O. Exploring the morphospace of communication efficiency in complex networks. *PLoS One* 8, 3. (2013): e58070.
- [69] Estrada, E., & Hatano, N. (2007). Statistical-mechanical approach to subgraph centrality in complex networks. *Chemical Physics Letters*, 439(1-3), 247-251.
- [70] R. Milo, S. Shen-Orr, S. Itzkovitz, et al., “Network motifs: simple building blocks of complex networks,” *Science* 298, 824–827 (2002).
- [71] Griffa, Alessandra, Philipp S. Baumann, Paul Klauser, Emeline Mullier, Martine Cleusix, Raoul Jenni, Martijn P. van den Heuvel, Kim Q. Do, Philippe Conus, and Patric Hagmann. Brain connectivity alterations in early psychosis: from clinical to neuroimaging staging. *Translational psychiatry* 9, no. 1 (2019): 1-10.
- [72] Crossley, N. A., Mechelli, A., Vertes, et al (2013). Cognitive relevance of the community structure of the human brain functional coactivation network. *Proceedings of the National Academy of Sciences*, 110(28), 11583-11588.
- [73] P. Yodzis, “Local trophodynamics and the interaction of marine mammals and fisheries in the Benguela ecosystem,” *J. Anim. Ecol.* 67, 635-658 (1998).
- [74] G. A. Polis, “Complex trophic interactions in deserts: an empirical critique of food-web theory,” *Am. Nat.* 138, 123-155 (1991).
- [75] C. Townsend, R. M. Thompson, and A. R. McIntosh, et al. Disturbance, resource supply, and food-web architecture in streams, *Ecol. Lett.* 1, 200 (1998).
- [76] R. R. Christian, and J. J. Luczkovich, “Organizing and understanding a winter’s seagrass foodweb network through effective trophic levels,” *Ecol. Model.* 117, 99-124 (1999).

- [77] P. H. Warren, "Spatial and temporal variation in the structure of a fresh-water food web," *Oikos* 55, 299-311 (1989).
- [78] R. B. Waide, and W. B. Reagan, (Eds.) *The Food Web of a Tropical Rainforest*. (University Chicago Press, Chicago, 1996).
- [79] N. D. Martinez, B. A. Hawkins, H. A. Dawah, and B. P. Feifarek, Effects of sampling efforts on characterization of food web structure, *Ecology* 80, 1044-1055 (1999).
- [80] K. Havens, Scale and structure in natural food webs, *Science* 257, 1107-1109 (1992).
- [81] S. Opitz, "Trophic Interactions in Caribbean coral reefs," ICLARM Tech. Rep. 43, Manila, Philippines, (1996).
- [82] J. Memmott, N. D. Martinez, and J. E. Cohen, Predators, parasites and pathogens: species richness, trophic generality, and body sizes in a natural food web, *J. Animal Ecol.* 69, 1-15 (2000).
- [83] J. Link, Does food web theory work for marine ecosystems?, *Mar. Ecol. Prog. Ser.* 230, 1-9 (2002).
- [84] P. Yodzis, "Diffuse effects in food webs," *Ecology* 81, 261-266 (2000).
- [85] L. Goldwasser, and J. A. Roughgarden, "Construction and analysis of a large Caribbean food web," *Ecology* 74, 1216-1233 (1993).
- [86] N. D. Martinez, Artifacts or attributes? Effects of resolution on the Little Rock Lake food web, *Ecol. Monogr.* 61, 367-392 (1991).
- [87] D. Baird, and R. E. Ulanowicz, The seasonal dynamics of the Chesapeake Bay ecosystem, *Ecol. Mon.* 59, 329-364 (1989).

- [88] M. Huxman, S. Beany, and D. Raffaelli, Do parasites reduce the chances of triangulation in a real food web?, *Oikos* 76, 284-300 (1996).
- [89] S. J. Hall, and D. Raffaelli, “Food-web patterns - lessons from a species-rich web,” *J. Anim. Ecol.* 60, 823–842 (1991).
- [90] A. Perna, S. Valverde, and J. Gautrais, et al. “Topological efficiency in the three-dimensional gallery networks of termite nests,” *Physica A* 387, 6235-6244 (2008).
- [91] Roget’s Thesaurus of English Words and Phrases, Project Gutenberg. <http://gutenberg.net/etext/22> (2002).
- [92] D. Bu, Y. Zhao, and L. Cai, et al. Topological structure analysis of the protein-protein interaction network in budding yeast, *Nucleic Acids Res.* 31, 2443-2450 (2003).
- [93] C. von Mering, R. Krause, and B. Snel, et al. Comparative assessment of large-scale data sets of protein-protein interactions, *Nature* 417, 399-403 (2002).
- [94] R. Milo, S. Itzkovitz, and N. Kashtan, et al. Superfamilies of evolved and designed networks, *Science* 303, 1538-1542 (2004).
- [95] S. Shen-Orr, R. Milo, S. Mangan, and U. Alon, Network motifs in the transcriptional regulation network of Escherichia coli, *Nature Gen.* 31, 64-68 (2002).
- [96] V. Batagelj, and A. Mrvar, Pajek datasets. Available at: <http://vlado.fmf.uni-lj.si/pub/networks/data/> (2006).
- [97] J. Leskovec, J. Kleinberg and C. Faloutsos. Graph Evolution: Densification and Shrinking Diameters. ACM Transactions on Knowledge Discovery from Data (ACM TKDD), 1(1), 2007.

- [98] J. Moody, Data for this project was provided in part by NIH grants DA12831 and HD41877, those interested in obtaining a copy of these data should contact James Moody (moody.77@sociology.osu.edu), (2001).
- [99] M. Faloutsos, P. Faloutsos, and C. Faloutsos, On power-law relationships of the internet topology, *Comp. Comm. Rev* 29, 251-262 (1999).
- [100] D. J. Watts, and S. H. Strogatz, Collective dynamics of small-world networks, *Nature* 393, 440-442 (1998).
- [101] C. R. Myers, Software systems as complex networks: Structure, function, and evolvability of software collaboration graphs, *Phys. Rev. E* 68, 046116 (2003).

Name	n	m
Benguela	29	191
BridgeBrook	75	542
Canton	108	707
Chesapeake	33	71
Coachella	30	241
Drugs	616	2012
Electronic1	122	189
Electronic2	252	399
Electronic3	512	819
ElVerde	156	1439
Collaboration CoGe	3621	9461
Collaboration QcGr	4158	13428
Internet1997	3015	5156
LittleRockA	181	2318
Neurons	280	1973
PIN_Yeast	2224	6608
Power_grid	4941	6594
ReefSmall	50	503
Roget	994	3640
ScotchBroom	154	366
Shelf	81	1451
Skipwith	35	353
Software_Abi	1035	1719
Software_Digital	150	198
Software_Mysql	1480	4140
Software_VTK	771	1357
Software_XMMS	971	1802
StMarks	48	218
StMartin	44	218
Stony	112	830
Termite_1	507	676
Termite_2	260	280
Termite_3	268	437
Transc_yeast	662	1062
USAir97	332	2126
Ythan1	134	593
Ythan2	92	416
Brain (task-driven)	638	18625
Brain (resting-state)	1000	10724 \pm 708

Table 2: Dataset of real-world networks studied in this paper, their size n (number of nodes), and number of edges m .